



**HAL**  
open science

## Random effects compound Poisson model to represent data with extra zeros

Marie-Pierre Etienne, Eric Parent, Benoit Hugues, Bernier Jacques

► **To cite this version:**

Marie-Pierre Etienne, Eric Parent, Benoit Hugues, Bernier Jacques. Random effects compound Poisson model to represent data with extra zeros. 2009. hal-00407962

**HAL Id: hal-00407962**

**<https://hal.science/hal-00407962>**

Submitted on 28 Jul 2009

**HAL** is a multi-disciplinary open access archive for the deposit and dissemination of scientific research documents, whether they are published or not. The documents may come from teaching and research institutions in France or abroad, or from public or private research centers.

L'archive ouverte pluridisciplinaire **HAL**, est destinée au dépôt et à la diffusion de documents scientifiques de niveau recherche, publiés ou non, émanant des établissements d'enseignement et de recherche français ou étrangers, des laboratoires publics ou privés.

# Random effects compound Poisson model to represent data with extra zeros

Marie-Pierre Étienne<sup>\*,a,b</sup>, Éric Parent<sup>a,b</sup>, Hugues Benoit<sup>c</sup>, Jacques Bernier<sup>a</sup>

<sup>a</sup>*AgroParisTech, UMR 518, F-75000 Paris, France*

<sup>b</sup>*INRA, UMR 518, F-75000 Paris, France*

<sup>c</sup>*Fisheries and Oceans Canada, Moncton, New Brunswick, Canada*

---

## Abstract

This paper describes a compound Poisson-based random effects structure for modeling zero-inflated data. Data with large proportion of zeros are found in many fields of applied statistics, for example in ecology when trying to model and predict species counts (discrete data) or abundance distributions (continuous data). Standard methods for modeling such data include mixture and two-part conditional models. Conversely to these methods, the stochastic models proposed here behave coherently with regards to a change of scale, since they mimic the harvesting of a marked Poisson process in the modeling steps. Random effects are used to account for inhomogeneity. In this paper, model design and inference both rely on conditional thinking to understand the links between various layers of quantities : parameters, latent variables including random effects and zero-inflated observations. The potential of these parsimonious hierarchical models for zero-inflated data is exemplified using two marine macroinvertebrate abundance datasets from a large scale scientific bottom-trawl survey. The EM algorithm with a Monte Carlo step based on importance sampling is checked for this model structure on a simulated dataset : it proves to work well for parameter estimation but parameter values matter when re-assessing the actual coverage level of the confidence regions far from the asymptotic conditions.

*Key words:* EM algorithm, Importance Sampling, Compound Poisson Process, Random Effect Model, zero-inflated Data

*2008 MSC:* 62F12, 62P12, 62L12, 92D40, 92d50

---

\* Département MMIP - Team Morse. 16 rue Claude Bernard, 75231 Paris Cedex 5. FRANCE  
*Email address:* [marie.etienne@agroparistech.fr](mailto:marie.etienne@agroparistech.fr) ()  
*URL:* [www.agroparistech.fr/morse/etienne.html](http://www.agroparistech.fr/morse/etienne.html) ()

## 1. Introduction

Often data contain a greater number of zero observations than would be predicted using standard, unimodal statistical distributions. This currently happens in ecology (see [16]) when counting species (over-dispersion for discrete data) or recording biomasses (atoms at zero for continuous data). Such data are generally referred to as zero-inflated data and require specialized treatments for statistical analysis [12]. Common statistical approaches to modeling zero-inflated data make recourse either to mixture models, such as the Dirac function for the occurrence of extra zeros in addition to a standard probability distribution (see for instance [21]), or to two-part conditional models (a presence/absence Bernoulli component and some other distribution for non zero observations given presence such as in [25]). These models are well-known [4] and offer the advantages of separate fits and separate interpretations of each of their components. Parameters are well understood and interpreted as the probability of presence, and the average abundance of biomass if present.

However, a major flaw of those models is their non-additive behavior with regards to variation in within-experiment sampling effort [26]. Consider for instance the fishing effort measured by the ground surface swept by a bottom-trawl during a scientific survey of benthic marine fauna. If during experiment  $i$ , observation  $Y_i$  is made with some experimental effort corresponding to the harvesting of some area  $D_i$  and is assumed to stem from a stochastic model with parameters  $\theta(D_i)$ , then the additivity properties of coherence are naturally required: if we consider two (possibly subsequent) independent experiments  $i$  and  $i'$  on the different non overlapping areas  $D_i$  and  $D_{i'}$ , we would expect that the random quantity  $Y_i + Y_{i'}$  stems from the same stochastic model with parameters  $\theta(D_i \cup D_{i'})$ . A compound Poisson distribution is a sum of independent identically distributed random variables in which the number of terms in the sum has a Poisson distribution. Compound Poisson distributions are candidate models purposely tailored to verify the previous desired infinite divisibility property since the class of infinitely divisible distributions coincides with the class of limit distributions of compound Poisson distributions ([9], theorem 3 of chapter 27).

Depending on the nature of the term in the random sum, the compound distribution can be discrete or continuous. The construction of such a compound distribution with an exponential random mark for continuous data and with a geometric one for counts is recalled in section 2. This approach is worthwhile for two reasons. The first is parsimony : there is only one parameter for the Poisson distribution plus an additional one for the probability distribution function - *pdf* - of each component of the random sum. Secondly, the compound construction may assist our understanding in cases where the data collection can be interpreted in terms of sampling a latent marked Poisson field. That is to say that the data

41 appear in latent "clumps" that are "harvested" during the experiment, the Pois-  
42 son parameter being the presence intensity of such clumps. A random variable  
43 is used to mimic the quantity (or the number of individuals in the discrete case)  
44 independently in each clump. At the upper level of the hierarchy, random effects  
45 are added to depict heterogeneous conditions between blocks of experiments.

46 In section 3, we develop a stochastic version of the EM algorithm [7] with a  
47 Monte-Carlo step (using importance sampling) for this non Gaussian random ef-  
48 fect model with zero-inflated data. Maximum likelihood estimates and the corre-  
49 sponding variance-covariance matrix are derived. The computational task remains  
50 rather tractable thanks to simplifying gamma-exponential conjugate properties in  
51 the continuous case (and beta-geometric conjugacy in the discrete case).

52 In section 4, the hierarchical model [29] with compound Poisson distribution for  
53 zero-inflated data is exemplified using a real case study with two marine species,  
54 urchin and starfish abundance data from a scientific bottom-trawl survey of the  
55 southern Gulf of St. Lawrence, Canada. The EM algorithm performs well in  
56 obtaining the maximum likelihood estimates of parameters, but for one of the  
57 two species we notice some discrepancy between the actual coverage of the con-  
58 fidence intervals and their theoretical levels (as given by the asymptotic normal  
59 approximation). Consequently, we further focus on variance covariance matrix es-  
60 timation in section 5 and investigate via simulation the behavior of coverage level  
61 of confidence intervals for various experimental designs, in search of a practical  
62 fulfillment of the asymptotic conditions. Finally, we briefly discuss some inferen-  
63 tial and practical issues encountered when implementing such hierarchical models  
64 for zero-inflated data.

## 65 2. Model construction

66 We propose a hierarchical construction to represent data with extra zero col-  
67 lected over a non-homogeneous area. The model is divided into two main layers :  
68 in the first one, we model the sampling process within a homogeneous sub-area  
69 (strata) and in the second layer, we introduce heterogeneity between strata at the  
70 top of the hierarchy using random effects. The first subsections detail the hierar-  
71 chical constructions for continuous data. In the last subsection 2.4, we sketch out  
72 an obvious modification to represent count data.

### 73 2.1. Compound Poisson process to introduce extra zeros

74 Imagine that data  $Y$  are obtained by harvesting an area  $D$  and that there are  
75 some clumps distributed according to an homogeneous Poisson process : clumps  
76 are uniformly distributed with a constant intensity, say  $\mu$ .

By harvesting an area  $D$ , we pick an integer-valued random variable  $N$  of  
clumps. According to Poisson process property  $N$  follows a Poisson distribution of

parameter  $\mu D$ . For each clump  $i$  the independent random variables  $X_i$  or *marks* (with the same probability distribution) represent for instance the possible biomass in each clump to be collected.

The final return will consist of the sum over  $N$  clumps of the amount contained in each clump. With the convention that  $Y = 0$  if  $N = 0$ , the random sum :

$$Y = \sum_{i=0}^N X_i, \quad (2.1)$$

77 is said to follow a compound Poisson distribution. Figure 1 exemplifies a realization  
78 of the total amount of a collect (i.e., sum of the marks) in a sampled region  $D$ .

79

80 The Poisson-based additivity property avoids the drawback of classical models  
81 mentioned in the introduction. Generally,  $D$  is the area of the sampled area  
82 included in  $\mathbb{R}^2$ . We assume an homogeneous region  $\mu(D) = \mu D$ , so that the  
83 expected number of collected clumps is proportional to the catching effort. The  
84 difficulty with the generalization to an inhomogeneous Poisson process lies in the  
85 inference step, not in the modeling step. Consequently we used another approach  
86 to deal with heterogeneity (see section 2.3). In the following, we mostly omit  
87 to index quantities with this catching effort for presentation clarity, explicitly  
88 mentioning it only when necessary.

89 Summary statistics about such compound distribution  $Y$  are easily obtained  
90 (the characteristic function is given in appendix A) :

$$\begin{aligned} \mathbb{E}(Y) &= \mu D \mathbb{E}(X) \\ \text{Var}(Y) &= \mu D \mathbb{E}(X^2) \end{aligned}$$

91 Parameter  $\mu$  rules the occurrence of zero values when assuming  $\mathbb{P}(X = 0) = 0$   
92 *i.e.* that the random mark is non atomic at 0 :

$$\mathbb{P}(Y = 0) = \exp(-\mu D).$$

### 93 2.2. Choice of the random component $X$ for continuous data

For real-valued data with extra zeros, we will concentrate in this paper on the exponential distribution of parameter  $\rho$  for component  $X$  such that  $\mathbb{E}(X) = \rho^{-1}$ , leading to

$$\mathbb{E}(Y) = \frac{\mu D}{\rho} \quad \text{and} \quad \text{Var}(Y) = 2 \frac{\mu D}{\rho^2}.$$

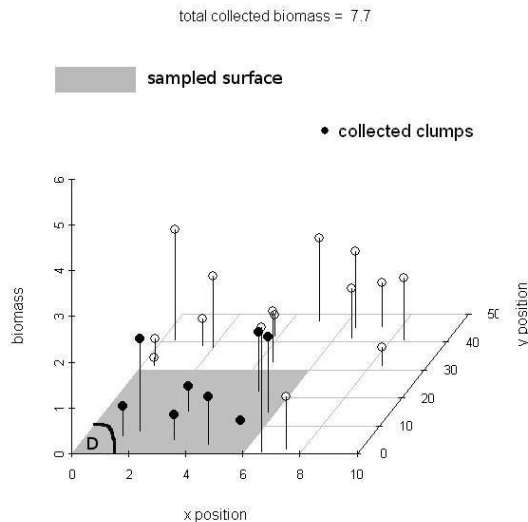


Figure 1: Realization of a marked Poisson process on a region of  $\mathbb{R}^2$ , the sample is conducted over a region  $D$ . Here the total catch is  $y = 7.7$ , the effective number of collected clumps is 8.

94 To keep on with an ecological interpretation of the model, assuming that the  
 95 mark  $X$  follows an exponential distribution of parameter  $\rho$ , means for the biologist  
 96 that the probability of finding a large amount of biomass within a clump is expo-  
 97 nentially decreasing and that the average quantity in each clump is  $\rho^{-1}$ . When  
 98 no clump is collected, there occurs a zero for the model  $Y$ . We choose the expo-  
 99 nential distribution because of parsimony and because of its interesting conjugate  
 100 property detailed in section 3.1.2.

This compound Poisson distribution was termed law of leaks (LOL) by [6], where  $X$  represents elementary unobserved leaks occurring at  $N$  holes (uniformly located) along a gas pipeline. In summary :

$$(Y \sim LOL(\mu, \rho)) \iff \left( \begin{array}{l} Y = \sum_{i=1}^N X_j, \\ N \sim \mathcal{P}(\mu), \\ (X_1, \dots, X_N) \stackrel{i.i.d}{\sim} \mathcal{E}(\rho) \end{array} \right) \quad (2.2)$$

101 For the discrete case, a similar definition holds with the corresponding geomet-  
 102 ric distribution for the marks (see section 2.4).

### 103 2.3. Random effects

Although the previous compound construction could have formally been extended to non-homogeneous Poisson processes, it is easier but still quite realistic to relax the assumption of homogeneity by considering homogeneous blocks (or

strata), modeling possible inter-block dispersion using random effects. We consider  $S$  blocks ; in a given block  $s$  there are  $I_s$  grouped observations. We denote by  $\underline{Y}_s = (Y_{s1}, \dots, Y_{sI_s})$  the random vector in block  $s$  and by  $\underline{\mathbf{Y}} = (\underline{Y}_1, \dots, \underline{Y}_S)$  the whole vector over the  $S$  blocks. The coefficients  $a$  and  $b$  of the gamma pdf  $\Gamma(a, b)$  for a random variable  $\mu$  are such that  $\mathbb{E}(\mu) = \frac{a}{b}$  and  $\text{Var}(\mu) = \frac{a}{b^2}$ . The random effect model  $RLOL(a, b, c, d)$  representing the occurrence of the sample  $\underline{\mathbf{Y}}$  is defined by the following set of equations.

$$\underline{\mathbf{Y}} \sim RLOL(a, b, c, d) \iff \begin{cases} (\mu_1, \dots, \mu_S) \stackrel{i.i.d}{\sim} \Gamma(a, b), \\ (\rho_1, \dots, \rho_S) \stackrel{i.i.d}{\sim} \Gamma(c, d), \\ Y_{s,1}, \dots, Y_{s,I_s} \mid \mu_s, \rho_s \stackrel{i}{\sim} LOL(\mu_s D_{s,k}, \rho_s) \quad \forall s \in \{1, \dots, S\}. \end{cases} \quad (2.3)$$

104 The choice of a gamma distribution for the random effect is motivated by conjugate  
 105 properties which are useful in the inference of the model. Section 4.1.3 will show  
 106 that it may also be quite a realistic distribution for some datasets. The hierarchical  
 107 construction is summed up by the directed acyclic graph (DAG as termed by [23])  
 108 in Figure 2.

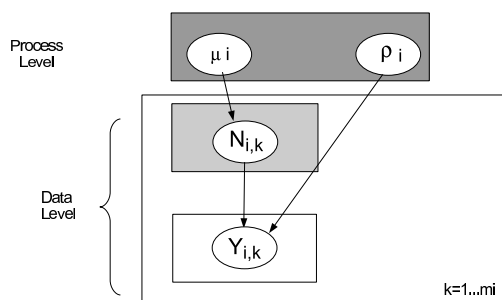


Figure 2: DAG of the RLOL model

#### 109 2.4. Compound Poisson process for count data

110 A similar but discrete version to model count data, can be obtained by changing  
 111 the nature of the random marks of the Poisson process. In this paper, we study  
 112 a geometric distribution with parameter  $p = \mathbb{P}(X = 1)$ . The core of the model is  
 113 thus given by the following compound Poisson process with geometric marks :

$$(Y \sim DLOL(\mu, p)) \iff \begin{pmatrix} Y = \sum_{j=1}^N X_j, \\ N \sim \mathcal{P}(\mu), \\ (X_1, \dots, X_N) \stackrel{i.i.d}{\sim} \mathcal{G}(p) \end{pmatrix}$$

To preserve conjugate properties, the gamma distribution for the random effect on the marks is replaced by a beta distribution so that the count data version of

the model is given by :

$$\underline{\mathbf{Y}} \sim RDLOL(a, b, c, d) \iff \begin{cases} (\mu_1, \dots, \mu_S) \stackrel{i.i.d}{\sim} \Gamma(a, b), \\ (p_1, \dots, p_S) \stackrel{i.i.d}{\sim} \beta(c, d), \\ Y_{s,1}, \dots, Y_{s,I_s} \mid \mu_s, p_s \stackrel{i}{\sim} DLOL(\mu_s D_{s,k}, p_s) \quad \forall s \in \{1, \dots, S\}. \end{cases} \quad (2.4)$$

114 where *DLOL* means Discrete version of Law of leaks and *RDLOL* discrete law of  
115 leaks with random effects.

116 In most of the paper, we will simply state the main results when technical  
117 aspects of the proofs are shared between discrete and continuous cases.

### 118 3. Estimation via the EM algorithm with importance sampling

119 Hierarchical models such as 2.3 or 2.4 cannot be straightforwardly estimated  
120 because of the latent variables. The random effects  $(\mu, \rho)$  and the unknown num-  
121 bers of clumps  $\underline{\mathbf{N}}$  must be integrated out to obtain the likelihood. The likelihood  
122 has no closed form and estimators cannot be directly derived. In such a case,  
123 a classical strategy is to use Expectation Maximization algorithm ([7]) to derive  
124 max-likelihood estimates. In our case the E step is not analytically accessible. An  
125 alternative is to use a stochastic version of this EM algorithm such as Monte-Carlo  
126 EM ( MCEM see [18] or [19]) or stochastic approximation of EM (SAEM see [8]).

127 We detail in this section how to implement a MCEM algorithm using Impor-  
128 tance sampling to obtain the maximum likelihood estimation and its empirical  
129 variance matrix. Similar results concerning count data process are summed up  
130 in the last subsection. From this point onwards we will use brackets to denote  
131 *pdf*'s as many conditioning terms will appear in the probabilistic expressions de-  
132 rived from the model fully specified by the set of equations (2.3). The brackets  
133 denote either a density or a discrete probability distribution, as in [10]. Following  
134 Bayesian conventions, we will also allow the parameters to appear as condition-  
135 ing terms (*i.e.*, instead of writing  $\mathbb{P}(X)$  we will specify  $[X|a, b, c, d]$ ) so as to help  
136 the reader understand which layer of the hierarchical model (2.3) the probability  
137 expression refers to (see Fig 2).

#### 138 3.1. Implementation of the MCEM algorithm

139 In this paper,  $\theta$  stands for the set of parameters  $(a, b, c, d)$  in the *RLOL* model.  
140 Given the random effects, the data within a block are independent :

$$L(\theta; \underline{\mathbf{Y}}, \underline{\mathbf{N}}, \mu, \rho) = \sum_{s=1}^S L_s$$

141 where  $L_s$  denotes the *complete* log-likelihood in block  $s$ , *i.e.* :



$$L_s = L_s(\theta; \underline{Y}_s, \underline{N}_s, \mu_s, \rho_s) = \left( \sum_{i=1}^{I_s} \ln ([Y_{s,i} | N_{s,i}, \rho_s] [N_{s,i} | \mu_s]) \right) + \ln([\mu_s | a, b]) + \ln([\rho_s | c, d]) \quad (3.1)$$

142 Following [28], the pivotal quantity in the EM algorithm (recalled in appendix  
143 D) is the conditional expectation of the complete log-likelihood :

$$Q(\theta, \theta') = \mathbb{E}_{\theta'} (L(\theta; \underline{\mathbf{Y}}, \underline{\mathbf{N}}, \mu, \rho) | \underline{\mathbf{Y}})$$

144 *3.1.1. Maximization step*

145 To maximize  $Q(\theta, \theta')$  with respect to  $\theta$ , we focus on the terms that involve  $\theta$  :

$$\begin{aligned} Q(\theta, \theta') = & C_{-\theta}(Y) + (a-1) \times \sum_{s=1}^S \mathbb{E}_{\theta'} (\ln \mu_s | \underline{Y}_s) + Sa \ln b - b \sum_{s=1}^S \mathbb{E}_{\theta'} (\mu_s | \underline{Y}_s) - S \ln(\Gamma(a)) \\ & + (c-1) \times \sum_{s=1}^S \mathbb{E}_{\theta'} (\ln \rho_s | \underline{Y}_s) + Sc \ln d - d \sum_{s=1}^S \mathbb{E}_{\theta'} (\rho_s | \underline{Y}_s) - S \ln(\Gamma(c)), \quad (3.2) \end{aligned}$$

146 where  $C_{-\theta}(Y)$  denotes a constant which does not depend on  $\theta$ .

147 Differentiating with respect to  $\theta$ , we obtain the set of equations to be satisfied  
148 at the maximum  $\underset{\theta}{\operatorname{argmax}} Q(\theta, \theta')$ :

$$\frac{a}{b} = \frac{\sum_{s=1}^S \mathbb{E}_{\theta'} (\mu_s | \underline{Y}_s)}{S} \quad (3.3)$$

$$\ln a - \psi(a) = \ln \left( \frac{\sum_{s=1}^S \mathbb{E}_{\theta'} (\mu_s | \underline{Y}_s)}{S} \right) - \frac{\sum_{s=1}^S \mathbb{E}_{\theta'} (\ln \mu_s | \underline{Y}_s)}{S} \quad (3.4)$$

$$\frac{c}{d} = \frac{\sum_{s=1}^S \mathbb{E}_{\theta'} (\rho_s | \underline{Y}_s)}{S} \quad (3.5)$$

$$\ln c - \psi(c) = \ln \left( \frac{\sum_{s=1}^S \mathbb{E}_{\theta'}(\rho_s | \underline{Y}_s)}{S} \right) - \frac{\sum_{s=1}^S \mathbb{E}_{\theta'}(\ln \rho_s | \underline{Y}_s)}{S} \quad (3.6)$$

149  $\psi(x)$  denotes the digamma function defined as the first logarithmic derivative  
 150 of  $\Gamma(x)$ . No analytical expression can be derived for  $\theta$  as the argument of the  
 151 maximum of  $Q(\theta, \theta')$ , but a Newton-Raphson algorithm is efficient and easy to  
 152 implement with a good empirical starting point as indicated in annex B.

### 153 3.1.2. Expectation step by conditioning onto the number of clumps

154 The right-hand side of equations 3.3 to 3.6 involves  $\mathbb{E}_{\theta'}(\mu_s | \underline{Y}_s)$ ,  $\mathbb{E}_{\theta'}(\ln(\mu_s) | \underline{Y}_s)$ ,  
 155  $\mathbb{E}_{\theta'}(\rho_s | \underline{Y}_s)$  and  $\mathbb{E}_{\theta'}(\ln(\rho_s) | \underline{Y}_s)$ . To compute these expected values, we will pro-  
 156 ceed by conditioning onto the hidden number of clumps  $\underline{\mathbf{N}}$ . Proposition 3.1 shows  
 157 that, given  $\underline{\mathbf{N}}$ , these four target quantities are simply marginal expectations of  
 158 the sufficient quantity  $N_{s+}$ , the only necessary function of  $\underline{\mathbf{N}}$  that needs to be  
 159 evaluated within each block  $s$ .

160 In a second step, integration over the number of clumps is performed by re-  
 161 course to importance sampling within a block  $s$  as detailed in proposition 3.3.  
 162 Proofs of propositions are given in appendix E

163 **Proposition 3.1.** *Assuming  $Y \sim RLOL(\theta')$  with  $\theta' = (a', b', c', d')$ ,  $S$  strata and*  
 164  *$I_s$  records in stratum  $s$  as in 2.3, then the complete conditional distributions of  $\mu_s$*   
 165 *and  $\rho_s$  in one particular stratum  $s$  are given by*

$$\mu_s | \underline{\mathbf{N}}, \underline{\mathbf{Y}}, \theta' \sim \Gamma(a' + N_{s+}, b' + D_{s+}), \quad (3.7)$$

166 and

$$\rho_s | \underline{\mathbf{N}}, \underline{\mathbf{Y}}, \theta' \sim \Gamma(a' + N_{s+}, b' + Y_{s+}), \quad (3.8)$$

167 where in stratum  $s$ ,  $N_{s+} = \sum_{i=1}^{I_s} N_{si}$  denotes the total number of clumps caught,  
 168  $Y_{s+} = \sum_{i=1}^{I_s} Y_{si}$  is the entire quantity harvested and  $D_{s+} = \sum_{i=1}^{I_s} D_{si}$  is the whole  
 169 catching effort.

170 The quantities involved in the E step are given by

$$\mathbb{E}_{\theta'} (\mu_s | \underline{y}_s) = \frac{a' + \mathbb{E}_{\theta'} (N_{s+} | \underline{y}_s)}{b' + D_{s+}}, \quad (3.9)$$

$$\mathbb{E}_{\theta'} (\ln(\mu_s) | \underline{y}_s) = \mathbb{E}_{\theta'} (\psi(a' + N_{s+}) | \underline{y}_s) - \ln(b' + D_{s+}), \quad (3.10)$$

$$\mathbb{E}_{\theta'} (\rho_s | \underline{y}_s) = \frac{c' + \mathbb{E}_{\theta'} (N_{s+} | \underline{y}_s)}{d' + Y_{s+}}, \quad (3.11)$$

$$\mathbb{E}_{\theta'} (\ln(\rho_s) | \underline{y}_s) = \mathbb{E}_{\theta'} (\psi(c' + N_{s+}) | \underline{y}_s) - \ln(d' + Y_{s+}). \quad (3.12)$$

171 This result merely comes from the conjugacy property between gamma and  
 172 Poisson distributions for  $\mu$  (gamma and exponential distribution concerning  $\rho$ ).  
 173 The moments of gamma and log gamma, beta and log beta distributions are re-  
 174 called in appendix C.

175 In order to go one step further into the calculus, we have to perform the integra-  
 176 tion over  $N_+$ . Proposition 3.2 gives the distribution of  $N_+ | Y_+, \theta$  up to a constant.  
 177 Subsequently, the integration over  $N_+$  will make recourse to importance sampling  
 178 as proposed in [15]. This Monte Carlo algorithm is detailed in proposition 3.3.

**Proposition 3.2.** *Assuming  $Y \sim RLOL(a, b, c, d)$  with  $S$  strata, and  $I_s$  records in stratum  $s$ , the conditional distribution of  $\underline{N}_s | \theta, \underline{y}_s$  is given (up to a constant  $K$ ) by*

$$[\underline{N}_s | \theta', \underline{y}_s] = K \left( \frac{\Gamma(a' + N_{s+}) \Gamma(c' + N_{s+})}{(b' + D_{s+})^{N_{s+}} (d' + Y_{s+})^{N_{s+}}} \right) \prod_{i=1, y_i > 0}^{I_s} \left( \frac{y_{si}^{N_{si}}}{\Gamma(N_{si}) \Gamma(N_{si} + 1)} \right) \prod_{i=1, y_i = 0}^{I_s} \delta(N_{si}) \quad (3.13)$$

179 To draw a sample according to the rather intricate looking distribution 3.13, an  
 180 importance sampling based algorithm is detailed in the following proposition for  
 181 one replicate (often termed *particle*). In order to obtain a  $G$ -sample, this procedure  
 182 is repeated for each block  $G$  times.

183 **Proposition 3.3** (Generate one particle in one particular stratum  $s$  according to  
 184 distribution 3.13). *A particle  $g$  is a vector  $(N_{s+}^{(g)}, N_{s1}^{(g)}, \dots, N_{sI_s}^{(g)})$  in a particular  
 185 stratum  $s$ . Omitting  $s$  to make the reading easier, we may assume with no loss of  
 186 generality that the first  $I^+$  terms are non zero and the  $I - I^+$  followings are the  
 187 zero ones. The algorithm to generate one particle  $g$  runs as follows:*

- 188 1. Generate  $N_i^{(g)} = 0$  wherever  $y_{i=0}$  for  $i = I - I^+ + 1, \dots, I$ .

2. Generate the value of the random sum  $N_+^{(g)}$  according to the importance distribution :

$$f_{IS}(N^+) \propto \left( \frac{1}{b' + D_+} \right)^{N^+} \left( \frac{Y^+}{d' + Y^+} \right)^{N^+} \frac{\Gamma(a' + N^+) \Gamma(c' + N^+)}{\left( \prod_{i=1}^{I^+} \Gamma\left(\frac{y_i}{Y^+} N^+ + 1\right) \right) \Gamma(N_+ - I_+ + 1)}$$

189

190

191

192

As the one dimensional importance distribution  $f_{IS}$  is a quickly decreasing function of  $N^+$ , its normalizing constant can be easily approximated and a bounded interval is used in practice as the support of  $N^+$ .

193

194

3. Generate each  $N_i^{(g)}$  for  $i = 1, \dots, I^+$  so that the vector  $(N_1^{(g)} - 1, \dots, N_{I^+}^{(g)} - 1)$  is distributed according to a multinomial distribution  $\mathcal{M}(N_+^{(g)} - I_+, (y_1/Y_+, \dots, y_{I^+}/Y_+))$ .

4. Associate to the vector  $(N_+^{(g)}, N_1^{(g)}, \dots, N_{I^+}^{(g)})$  generated at the previous step, the importance weight :

$$w^{(g)} = \prod_{i=1}^{I_+} \frac{\Gamma\left(N_+^{(g)} \frac{y_i}{Y_+} + 1\right)}{\Gamma(N_i^{(g)} + 1)}$$

195

196

197

The proof of this proposition is straightforward from importance sampling theory (see for instance chapter 3 of [22]).

The weighted sample of  $N_+$  may be used to approximate the expected conditional value defined in equations 3.9 to 3.12. For instance, quantity 3.10 is approximated by :

$$\mathbb{E}_{\theta'}(\ln(\mu_s) \mid \underline{y}_s) \approx \left( \frac{1}{\sum_{g=1}^G \omega^{(g)}} \sum_{g=1}^G \omega^{(g)} \times \psi(a' + N_{s+}^{(g)}) \right) - \ln(b' + D_{s+}).$$

198

199

200

201

202

203

204

205

### 3.1.3. Empirical Variance Matrix

This section is devoted to the evaluation of the empirical variance matrix, so as to provide confidence regions. Because of the EM principle, we assume that the algorithm has converged to the maximum likelihood value  $\hat{\theta}$ . The empirical Fisher information matrix is then given by proposition 3.4. To explicitly compute this information matrix, we propose to numerically integrate over  $\underline{\mathbf{N}}$  thanks to importance sampling as performed for the point estimation step. Technical details are also given in appendix F.

**Proposition 3.4.** Assuming  $Y \sim RLOL(a, b, c, d)$  with  $S$  strata, and  $I_s$  records in stratum  $s$  as in 2.3. Let us denote  $I_e(\theta)$  the empirical information matrix defined by

$$I_e(\theta) = -\frac{\partial^2 \ln [\underline{\mathbf{Y}}|\theta]}{\partial \theta_i \partial \theta_j} \quad (3.14)$$

At the maximum likelihood estimator  $\hat{\theta}$ , the following equality holds :

$$I_e(\hat{\theta}, \underline{\mathbf{Y}}) = S \begin{pmatrix} -\psi'(\hat{a}) & \frac{1}{\hat{b}} & 0 & 0 \\ \frac{1}{\hat{b}} & -\frac{\hat{a}}{\hat{b}^2} & 0 & 0 \\ 0 & 0 & -\psi'(\hat{c}) & \frac{1}{\hat{d}} \\ 0 & 0 & \frac{1}{\hat{d}} & -\frac{\hat{c}}{\hat{d}^2} \end{pmatrix} + \sum_{s=1}^S (A_s + B_s) \quad (3.15)$$

206 with

$$A_s = \begin{pmatrix} \mathbb{E}_{\nu_s}(\psi'(a_s^*)) & \frac{-1}{b_s^*} & 0 & 0 \\ \frac{-1}{b_s^*} & \frac{\mathbb{E}_{\nu_s}(a_s^*)}{(b_s^*)^2} & 0 & 0 \\ 0 & 0 & \mathbb{E}_{\nu_s}(\psi'(c_s^*)) & \frac{-1}{d_s^*} \\ 0 & 0 & \frac{-1}{d_s^*} & \frac{\mathbb{E}_{\nu_s}(c_s^*)}{(d_s^*)^2} \end{pmatrix}$$

207 and

$$B_s = \begin{pmatrix} \text{Var}_{\nu_s}(\psi(a_s^*)) & -\frac{\text{Cov}_{\nu_s}(a_s^*, \psi(a_s^*))}{b_s^*} & \text{Cov}_{\nu_s}(\psi(a_s^*), \psi(c_s^*)) & -\frac{\text{Cov}_{\nu_s}(c_s^*, \psi(a_s^*))}{d_s^*} \\ -\frac{\text{Cov}_{\nu_s}(a_s^*, \psi(a_s^*))}{b_s^*} & \frac{\text{Var}_{\nu_s}(a_s^*)}{b_s^{*2}} & -\frac{\text{Cov}_{\nu_s}(a_s^*, \psi(c_s^*))}{b_s^*} & \frac{\text{Cov}_{\nu_s}(a_s^*, c_s^*)}{b_s^* d_s^*} \\ \text{Cov}_{\nu_s}(\psi(a_s^*), \psi(c_s^*)) & -\frac{\text{Cov}_{\nu_s}(a_s^*, \psi(c_s^*))}{b_s^*} & \text{Var}_{\nu_s}(\psi(c_s^*)) & -\frac{\text{Cov}_{\nu_s}(c_s^*, \psi(c_s^*))}{d_s^*} \\ -\frac{\text{Cov}_{\nu_s}(c_s^*, \psi(a_s^*))}{d_s^*} & \frac{\text{Cov}_{\nu_s}(a_s^*, c_s^*)}{b_s^* d_s^*} & -\frac{\text{Cov}_{\nu_s}(c_s^*, \psi(c_s^*))}{d_s^*} & \frac{\text{Var}_{\nu_s}(c_s^*)}{d_s^{*2}} \end{pmatrix},$$

208 where  $a_s^* = \hat{a} + N_{s+}$ ,  $b_s^* = \hat{b} + D_{s+}$ ,  $c_s^* = \hat{c} + N_{s+}$ ,  $d_s^* = \hat{d} + Y_{s+}$  and  $\nu_s$  stands  
209 for the probability measure of  $N_{s+}|\hat{\theta}, \underline{\mathbf{Y}}$ .

210 As for the first derivative phase of the EM algorithm detailed in section 3.3,  
211 the operations  $\mathbb{E}_{\underline{\mathbf{N}}|\hat{\theta}, \underline{\mathbf{Y}}}$  and  $\text{Var}_{\underline{\mathbf{N}}|\hat{\theta}, \underline{\mathbf{Y}}}$ , needed to evaluate  $A_s$  and  $B_s$ , can be eas-  
212 ily implemented by recourse to the very same Monte-Carlo  $N_+$  sample that was  
213 previously drawn by importance sampling.

#### 214 3.1.4. Prediction of the random effects

215 It is of interest to predict the random effects in each stratum, for instance to  
216 help illustrate the heterogeneity between units. In a linear mixed model context,  
217 the *Best Linear Unbiased Estimator* is defined by the conditional expectation of  
218 the random effect according to the data  $\underline{\mathbf{y}}$  and the point estimation. We follow

219 the same avenue of thought and define a predictor of the random effects by the  
 220 conditional expectation. Using formula 3.9 and 3.11, the random effect predictors  
 221 are given by :

$$\mu_s^{(pred)} = \mathbb{E}(\mu_s | \underline{y}, \hat{\theta}) = \frac{\hat{a} + \mathbb{E}(N_{s+} | \underline{y}_s, \hat{\theta})}{\hat{b} + D_{s+}}, \quad (3.16)$$

222 and

$$\rho_s^{(pred)} = \mathbb{E}(\rho_s | \underline{y}, \hat{\theta}) = \frac{\hat{c} + \mathbb{E}(N_{s+} | \underline{y}_s, \hat{\theta})}{\hat{d} + Y_{s+}}, \quad (3.17)$$

223 The following section aims at highlighting the differences between the contin-  
 224 uous case detailed previously and the discrete one.

### 225 3.2. MCEM algorithm for RDLOL model

#### 226 3.2.1. Straightforward transposition to the discrete case

227 The definition of the model designed for the discrete case and called RDLOL  
 228 model is given by equation 2.4, in this case the pivotal quantity  $Q(\theta, \theta')$  reads :

$$\begin{aligned} Q(\theta, \theta') = & C_{-\theta}(Y) + (a-1) \sum_{s=1}^S \mathbb{E}_{\theta'}(\ln \mu_s | \underline{Y}_s) + Sa \ln b - b \sum_{s=1}^S \mathbb{E}_{\theta'}(\mu_s | \underline{Y}_s) - S \ln(\Gamma(a)) \\ & + \ln \left( \frac{\Gamma(c+d)}{\Gamma(c)\Gamma(d)} \right) + (c-1) \sum_{s=1}^S \mathbb{E}_{\theta'}(\ln p_s | \underline{Y}_s) + (d-1) \sum_{s=1}^S \mathbb{E}_{\theta'}(\ln(1-p_s) | \underline{Y}_s) \end{aligned} \quad (3.18)$$

229

The equations satisfied at the maximum for  $(a, b)$  are again 3.3 and 3.4. Due to the substitution of a gamma *pdf* into a beta *pdf* for the random effects governing the geometric discrete marks in the random sum of counts, parameters  $c$  and  $d$  verify equations 3.19 and 3.20 (equivalent to equations 3.5 and 3.6 in the continuous data model) :

$$\psi(c+d) - \psi(c) = - \frac{\sum_{s=1}^S \mathbb{E}_{\theta'}(\ln p_s | \underline{Y}_s)}{S} \quad (3.19)$$

$$\psi(c) - \psi(d) = \frac{\sum_{s=1}^S \mathbb{E}_{\theta'} \left( \ln \left( \frac{p_s}{1-p_s} \right) \middle| \underline{Y}_s \right)}{S} \quad (3.20)$$

230 The approach used for the continuous case is reproduced to obtain, in each stratum  $s$  the conjugate conditional density of  $\underline{\mu}, \underline{p}$ , so that the analog to propositions  
 231 3.1 and 3.2 is :  
 232

**Proposition 3.5.** *Assuming  $Y \sim RDLOL(\theta')$  with  $\theta' = (a', b', c', d')$ ,  $S$  strata and  $I_s$  records in stratum  $s$  as in 2.4, then the complete conditional distributions of  $\mu_s$  and  $p_s$  in one particular stratum  $s$  are given by*

$$\mu_s | N_{s+}, \theta' \sim \Gamma(a' + N_{s+}, b' + D_{s+}), \quad (3.21)$$

and

$$p_s | N_{s+}, \theta' \sim \beta(c' + N_{s+}, d' + Y_{s+} - N_{s+}). \quad (3.22)$$

233

Furthermore the conditional distribution function of  $\underline{N}_s$  is :

$$[\underline{N}_s | \theta', \underline{Y}] \propto \left( \prod_{i=1}^{I^+} \frac{\binom{Y_{si} - 1}{N_{si} - 1} D_{si}^{N_{si}}}{N_{si}!} \right) \left( \prod_{i=I-I^++1}^I \delta(N_{si}) \right) \left( \frac{\Gamma(a' + N_{s+}) \Gamma(N_{s+} + c') \Gamma(Y_+ - N_{s+} + d')}{(b' + D_{s+})^{N_{s+}}} \right) \quad (3.23)$$

234 The choice of an efficient importance sampling distribution in the discrete case  
 235 is not the straightforward adaptation of the continuous gives and a mixture has to  
 236 be used to obtain an efficient and well behaved algorithm, detailed in appendix H.

### 237 3.2.2. The covariance matrix in the discrete case

238 The covariance matrix in the discrete case benefits from the same conditional  
 239 independence decompositions and the adaptation of the continuous case is straight-  
 240 forward given the moments of the beta distribution in appendix C; the result is  
 241 detailed in appendix G. The weighted sample of  $N_+$  is used to compute the expect-  
 242 ations and variance-covariance terms in the matrix components.

### 243 3.2.3. Prediction of the random effects

244 The predictions of the random effects are just given by the conditional expect-  
 245 ations. Unsurprisingly, the predictions in the discrete case and in the continuous  
 246 one look very similar.  $\mu_s^{(pred)}$  is still given by formula 3.16 and

$$p_s^{(pred)} = \mathbb{E}(p_s | \underline{y}, \hat{\theta}) = \frac{\hat{c} + \mathbb{E}\left(N_{s+} | \underline{y}_s, \hat{\theta}\right)}{\hat{c} + \hat{d} + Y_{s+}}, \quad (3.24)$$

## 247 4. Applications

248 In this section, we apply the EM estimation procedure to two real datasets  
249 of ecological interest. We then study the validity of asymptotic assumptions by  
250 assessing the coverage level of confidence regions.

### 251 4.1. Real dataset - Gulf of St.Lawrence survey

252 A multi-species bottom-trawl survey of the southern Gulf of St.Lawrence (NW  
253 Atlantic) has been conducted each September since 1971. The purpose of this  
254 survey is to estimate the abundance and characterize the geographic distribution  
255 of marine biota. The survey follows a stratified random design, with 38 strata  
256 defined largely as homogeneous habitats using depth, temperature and sediments  
257 properties. The target fishing procedure at each fishing station is a 30-min straight-  
258 line tow at a speed of 3.5 knots (i.e., 3.21km trawled distance). However the actual  
259 distance trawled can vary due to winds, currents and the avoidance of damaging  
260 rough bottoms; sampling effort is therefore variable among trawl tows, but this  
261 source of additional variability is easily accommodated in the models presented  
262 here ( the  $D_{s,k}$  in eq 2.3). For our case study, we use data on the abundance of sea  
263 urchins and Sunflower starfishes collected during three survey years (1999-2001),  
264 in a total of 540 bottom-trawl sets. The time period was chosen to minimize  
265 inter-annual changes in abundance while ensuring a sufficient sample size. The  
266 species were selected because inter-annual changes in their geographic distribution  
267 resulting from movements of individuals at the scale of survey sampling can be  
268 assumed to be approximately nil.

269 The histograms of urchin and starfish catches in kg per survey tow clearly reflect  
270 zero-inflated distributions (Fig 3 and 4). A large number of tows capture no urchin  
271 (nor starfish) and catches in non-zero tows tend to follow a skewed distribution. At  
272 the scale of the survey, sea urchins are distributed in patches of localized variable  
273 abundance, interspersed by numerous and relatively large areas where the species  
274 is absent (Fig 5). Such *patchy* distributions of organisms are prevalent in ecological  
275 science. Data in two strata are always zero, thus rendering estimation impossible  
276 if we were to fit one model per stratum or to consider  $\rho_s$  as fixed effects. Because  
277 the hierarchical framework allows some transfer of information between strata, the  
278 other data help to predict  $\rho$  in these two strata.

#### 279 4.1.1. Maximum likelihood point estimation

The estimation procedure follows the EM algorithm detailed in appendix D  
(with a stopping rule when the sixth decimal does not change between iterations)  
and gives values of

$$\hat{\theta}^{Urch} = (\hat{a}, \hat{b}, \hat{c}, \hat{d}) = (0.997797, 1.05107, 5.05733, 13.0312),$$



**Urchins Biomass empirical distribution**

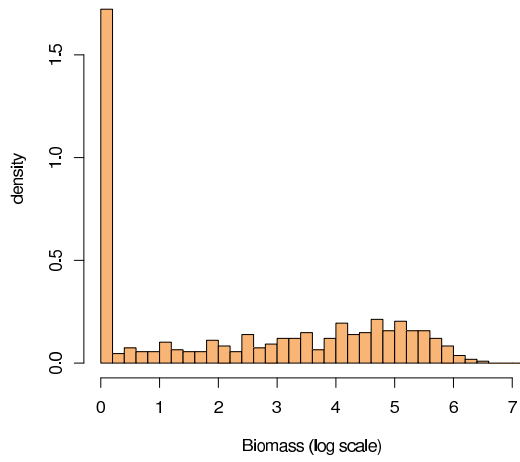


Figure 3: Histogram of urchin biomass (kg/tow) from individual tows in the southern Gulf of St. Lawrence, bottom-trawl surveys: 1999-2000-2001

**Sunflower starfishes Biomass empirical distribution**

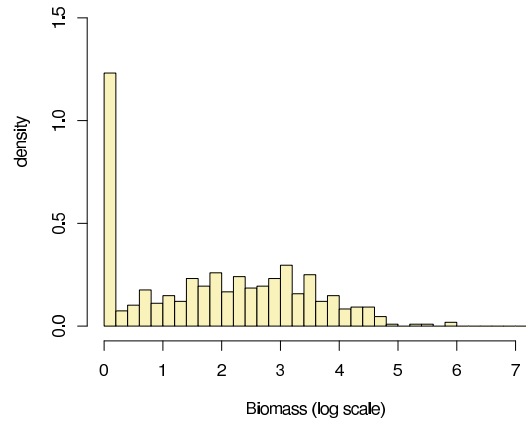


Figure 4: Histogram of Sunflower Starfishes biomass (kg/tow) from individual tows in the southern Gulf of St. Lawrence, bottom-trawl surveys: 1999-2000-2001

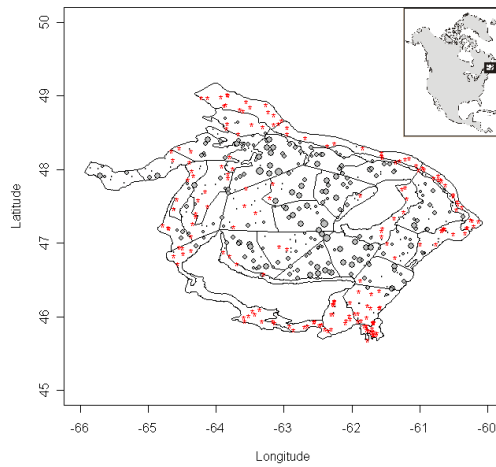


Figure 5: Locations of urchin catches (symbols) and stratum boundaries (lines) in the southern Gulf of St. Lawrence bottom-trawl surveys 1999-2000-2001. The radii of the circles are proportional to the biomass (in kg/tow) caught. The "\*" denote sites with no urchins caught. Starfishes are not plotted.

and

$$\hat{\theta}^{Sun} = (\hat{a}, \hat{b}, \hat{c}, \hat{d}) = (1.91879, 1.80704, 1.90002, 0.898734),$$

280 as a maximum likelihood point estimates respectively for Urchin and Sunflower  
 281 starfishes datasets.

282 A visual diagnosis of the goodness of fit is very informative. According to  
 283 the RLOL model, data are drawn from a mixture and we cannot add directly  
 284 a density line on the histograms of figures 3 and 4 since the zero ordinate of  
 285 these figures is somewhat artificial : it depends on the width of the histogram  
 286 bins and has been chosen so that the overall cumulative greyed surface is 100%.  
 287 The expected histograms presented in figures 6 and 7 have been obtained using  
 288 1000 replications of the model with the same design at  $\hat{\theta}$ , and averaging the 1000  
 289 generated histograms. Obviously the obtained model histogram (averaging all the  
 290 random effects) is smoother than the empirical distribution. The observed number  
 291 of zeros falls below the expected number but within the 90% confidence interval  
 292 for each species (as indicated by the vertical line on figures 6 and 7) and the overall  
 293 shape of the distribution fits quite well the data in both cases.

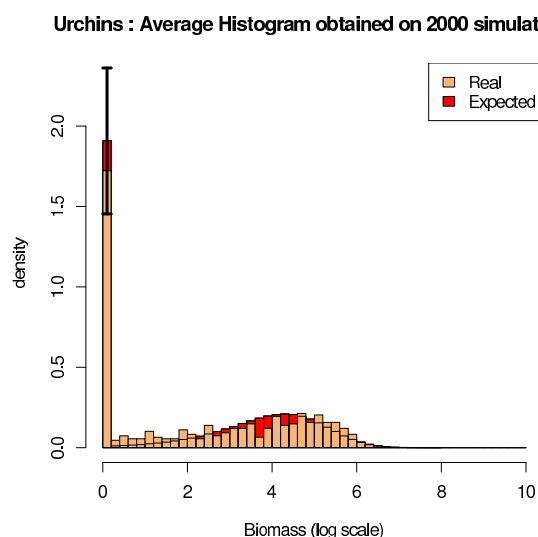


Figure 6: Comparisons between urchins dataset and averaged histogram (1000 simulations of datasets at  $\hat{\theta}^{Urch}$ )

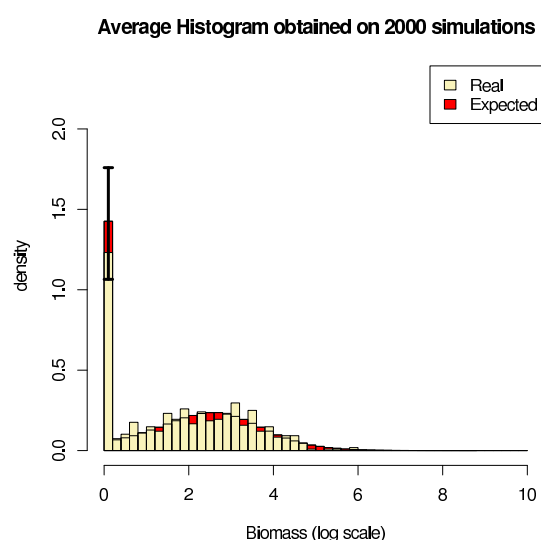


Figure 7: Comparisons between Sunflower Starfishes dataset and averaged histogram (1000 simulated datasets at  $\hat{\theta}^{Sun}$ )

294 4.1.2. Confidence intervals

Relying on proposition 3.4, the asymptotic covariance matrices are evaluated at those maximum likelihood arguments :

$$\begin{pmatrix} \text{var}(\hat{a}^{Urch}, \underline{\mathbf{Y}}) \\ \text{var}(\hat{b}^{Urch}, \underline{\mathbf{Y}}) \\ \text{var}(\hat{c}^{Urch}, \underline{\mathbf{Y}}) \\ \text{var}(\hat{d}^{Urch}, \underline{\mathbf{Y}}) \end{pmatrix} = \begin{pmatrix} 0.0587 \\ 0.1020 \\ 1.6804 \\ 14.4793 \end{pmatrix}$$

$$\text{Corr}(\hat{\theta}^{Urch}, \underline{\mathbf{Y}}) = \begin{pmatrix} 1 & 0.825 & 0.035 & 0.058 \\ 0.825 & 1 & 0.036 & 0.081 \\ 0.035 & 0.036 & 1 & 0.936 \\ 0.058 & 0.081 & 0.936 & 1 \end{pmatrix}$$

and

$$\begin{pmatrix} \text{var}(\hat{a}^{Sun}, \underline{\mathbf{Y}}) \\ \text{var}(\hat{b}^{Sun}, \underline{\mathbf{Y}}) \\ \text{var}(\hat{c}^{Sun}, \underline{\mathbf{Y}}) \\ \text{var}(\hat{d}^{Sun}, \underline{\mathbf{Y}}) \end{pmatrix} = \begin{pmatrix} 0.2555 \\ 0.3003 \\ 0.2609 \\ 0.0894 \end{pmatrix}$$

$$\text{Corr}(\hat{\theta}^{Sun}, \underline{\mathbf{Y}}) = \begin{pmatrix} 1 & 0.902 & -0.055 & -0.046 \\ 0.902 & 1 & -0.056 & -0.023 \\ -0.055 & -0.056 & 1 & 0.906 \\ -0.046 & -0.023 & 0.906 & 1 \end{pmatrix}$$

295 Essentially only  $\hat{a}$  and  $\hat{b}$  (resp  $\hat{c}$  and  $\hat{d}$ ) are correlated.

296 To evaluate the actual coverage of confidence regions in the present sampling  
 297 conditions (that may be far from asymptotics), 16000 simulations were launched,  
 298 assuming the same number of strata and the same number of data points per  
 299 stratum as the urchin catches (resp. sunflower starfishes) with  $\hat{\theta}$  as hypothetic true  
 300 parameter, thus disregarding possible bias. As a practical working conclusions,  
 301 Figures 8 and 9 show how to correct theoretical asymptotical confidence intervals.  
 302 The results are quite different from one dataset to the other.

- 303 • On Urchins dataset, to get an actual 90% confidence region, we must ex-  
 304 pand as far as the asymptotic ellipse corresponding to a 99.964% normal  
 305 approximation as shown in Figure 8.
- 306 • On Sunflower Starfish dataset, things work better and the 94% asymptotical  
 307 confidence interval is quite a good surrogate for an actual 90% confidence  
 308 region!

309 To understand Table 1, we suggest to consider the median column as the refer-  
 310 ence confidence interval (based on simulation/ EM re-estimation). The right col-  
 311 umn gives bootstrap+ EM re-estimation. We notice that the Bootstrap approach

| 90% Confidence Intervals |                      |                     |
|--------------------------|----------------------|---------------------|
| (asymptotic)             | (via simulation)     | (via bootstrap)     |
| Urchins case             |                      |                     |
| $0.587 < a < 1.384$      | $0.335 < a < 1.637$  | $0.72 < a < 1.00$   |
| $0.496 < b < 1.547$      | $0.163 < b < 1.880$  | $0.61 < b < 1.03$   |
| $2.827 < c < 7.092$      | $1.476 < c < 8.443$  | $1.23 < c < 4.37$   |
| $6.387 < d < 18.905$     | $2.419 < d < 22.872$ | $1.68 < d < 10.89$  |
| Starfishes case          |                      |                     |
| $1.087 < a < 2.750$      | $1.294 < a < 2.951$  | $1.217 < a < 1.859$ |
| $0.905 < b < 2.708$      | $1.198 < b < 3.141$  | $0.938 < b < 1.663$ |
| $1.059 < c < 2.740$      | $1.344 < c < 3.182$  | $1.147 < c < 2.035$ |
| $0.406 < d < 1.390$      | $0.558 < d < 1.559$  | $0.347 < d < 0.858$ |

Table 1: Comparison of the asymptotic 90% confidence interval with the one obtained by simulation for each parameter component for both species

312 is completely inappropriate for our model. The estimation is clearly biased with a  
313 shift to the right (verified on simulations not shown here) although we tried to cor-  
314 rect bias as proposed in [13]. The width of confidence intervals are underestimated  
315 for both species and does not even contain the  $\hat{\theta}$ -value. The hierarchical structure  
316 of the model may explain part of this bad behavior of bootstrap method but this  
317 would need further investigations not in the scope of this paper. The left column  
318 of Table 1 exhibits two different behaviors according to the species considered.

- 319 • The asymptotic variance of maximum likelihood parameters under-estimate  
320 strongly the true sampling characteristics in the Urchin case. This may be  
321 due to the large numbers of zero's for that species: consequently relatively  
322 less non zero data remain for the  $\rho$ 's (inverse of patch abundance) and the  
323 estimation of  $c$  and  $d$  that rule the between units variation of  $\rho$ 's may become  
324 difficult.
- 325 • The Sunflower Starfishes case exhibits much better properties regarding the  
326 approximation of the covariance matrix. For this species, less zeros data  
327 occur and we guess that enough information is made available in the sample  
328 to get correct estimations.

329 Figures 10 and 11 present the predictions for the random effects in each stratum.  
330

#### 331 4.1.3. Validation of the gamma assumption for random effects

332 We have assumed that the random effects  $\mu$  and  $\rho$  were distributed according to  
333 gamma distributions. This choice was essentially made for technical convenience

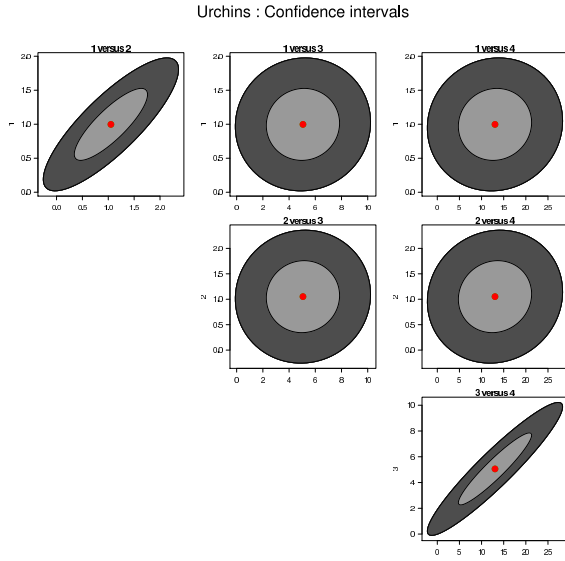


Figure 8: The lightest ellipse corresponds to 90% confidence ellipsoid and the darkest one is 99.96% and contains 90% of the simulated values.

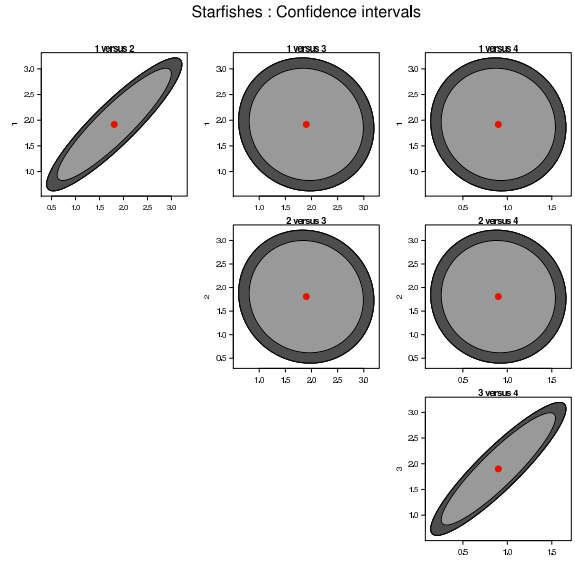


Figure 9: The lightest ellipse corresponds to 90% confidence ellipsoid and the darkest one is 94% and contains 90% of the simulated values.

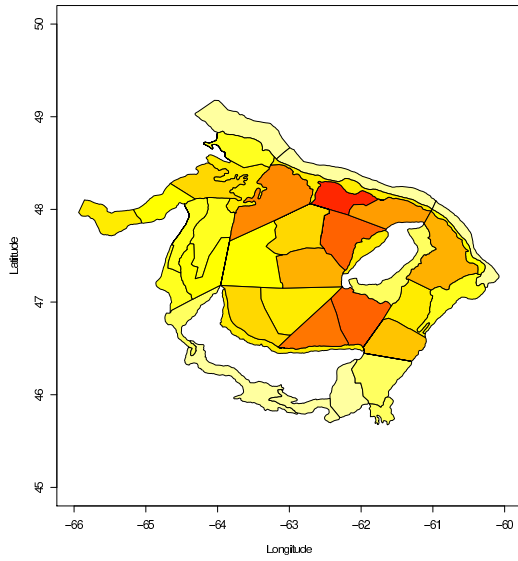


Figure 10: Predictions of the random effects  $\mu_s$  in each stratum correspond to the expected number of clumps collected during a measurement with standard catching effort.

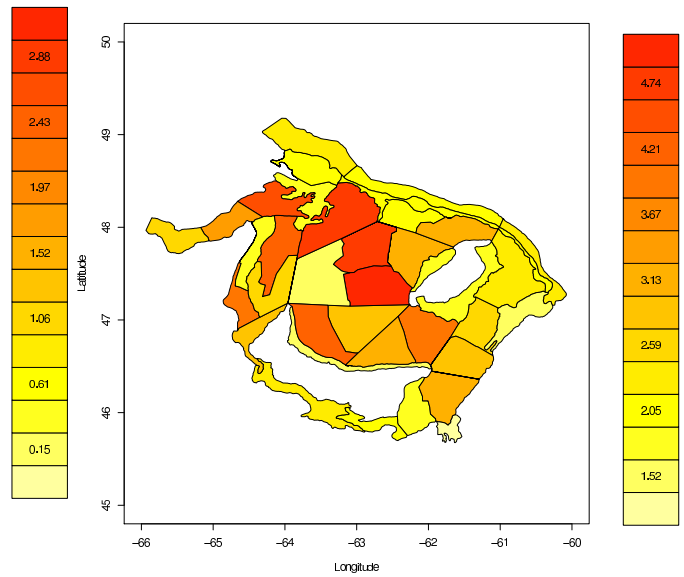


Figure 11: Predictions of the inverse of  $\rho_s$  in each stratum. These quantities give the expected biomass to be collected within a clump.

334 because conjugate properties make the estimation easier. The validity of this  
 335 assumption can be checked by considering random effects as fixed and estimate  
 336 them independently in each stratum. Figures 12 and 13 present a pp-plot of  
 337 empirical versus estimated probability distributions for  $\mu$  and  $\rho$ .

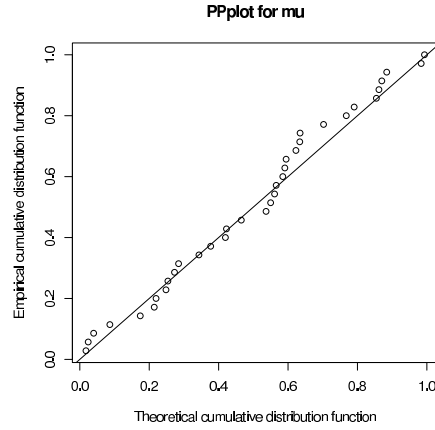


Figure 12: pp-Plot with estimates of  $\mu_s$  versus a fitted gamma distribution.

338 The pp-plot for  $\mu$  suggests that the gamma distribution is appropriate (Fig 12);  
 339 this is not true of the gamma pp-plot for  $\rho$  (Fig 13). First there are only 36 points  
 340 estimates because 2 strata are empty and  $\rho$ 's for these strata are not defined.  
 341 Second the probability plot does not adjust to a straight 45 degrees line. Looking  
 342 more closely at four extreme points in the  $\rho$  pp-plot, we found that they come from  
 343 strata with less than two non-zero data points. Excluding these 4 points produces  
 the much more acceptable fit of Figure 14.

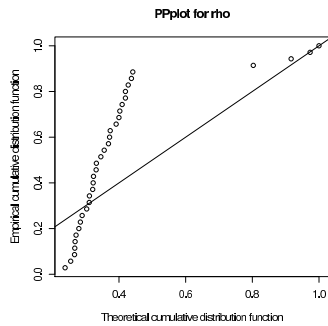


Figure 13: pp-Plot with estimates of  $\rho_s$  versus a fitted gamma distribution. The extremal points correspond to strat with at least 75% of zeros

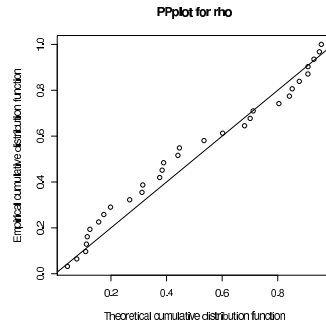


Figure 14: pp-Plot with estimates of  $\rho_s$  against a fitted gamma distribution after excluding the four outliers.

344

345 *4.2. Simulations Studies*

346 The previous section showed different behaviors depending on the species : the  
347 EM procedure provides rather reliable estimates for the starfish RLOL statistical  
348 features but not for the Urchin ones. The purpose of this section is to check the  
349 role of the sampling designs. Simulation studies are performed to explore the  
350 quality of the EM estimation procedure and to check the actual coverage of the  
351 asymptotic variance-covariance matrix approximation.

352 *4.2.1. Simulation design*

353 For a given set of parameters  $\theta = (a, b, c, d)$ , we draw 1000 samples according  
354 to RLOL model given in eq 2.3 with a number  $S$  of strata and  $M$  measured points  
355 per each stratum.  $S$  has been chosen varying as  $k^2$  with  $k = 3, 4, 5, 6, 8, 10, 12, 15$   
356 and  $M = 5, 10, 15, 20, 25, 30, 40$ .

357 For each simulation, the estimation procedure depicted in section 3 yields one  
358 point estimate and one estimation of the asymptotic covariance matrix. Assuming  
359 that the asymptotic approximation holds and using a normal approximation, con-  
360 fidence intervals can be given for the *true* value. As we work within a simulation  
361 context, the *true* value is known and one can compute the actual proportion of  
362 samples for which the asymptotic confidence interval covers the *true* value.

363 *4.2.2. RLOL Results*

364 The simulation study is achieved for two values of parameters  $\theta$  corresponding  
365 to the two applications developed in section 4.1. We choose  $\theta^{Urchin} = (1, 1, 5, 13)$   
366 and  $\theta^{Sunstars} = (1.9, 1.8, 1.9, 0.9)$  as *true* parameter references for the simulations.  
367 We first present a study of the bias and then an investigation of the actual coverage  
368 of confidence intervals.

369 **Bias study**

370 We can study the bias by simulation according to the numbers of strata and the  
371 number of measure points within strata. Figures 15 and 16 present the results for  
372 relative bias obtained with 1000 simulations in each configuration. As expected  
373 it decreases quickly with the number of strata and only marginal amelioration is  
374 obtained as soon as the number of data per stratum becomes reasonable.

375 **Confidence intervals study**

376 Using 1000 simulations in each cell, the empirical proportion of the asymptotic  
377 90% confidence ellipsoids that cover the *true* value is given in Figures 17 and 18.  
378 With 1000 trials in a binomial distribution with probability  $p$  of success, a confi-  
379 dence interval for  $p = 0.90$  is approximatively [88%, 92%] : cells from Figures 17  
380 and 18 that belongs to that interval have been colored in light grey. Results about  
381 confidence intervals strongly depend on the value of  $\theta$ . The asymptotic approxima-  
382 tion seems quite satisfying for  $\theta^{Sunstars}$  : the asymptotical conditions are quickly

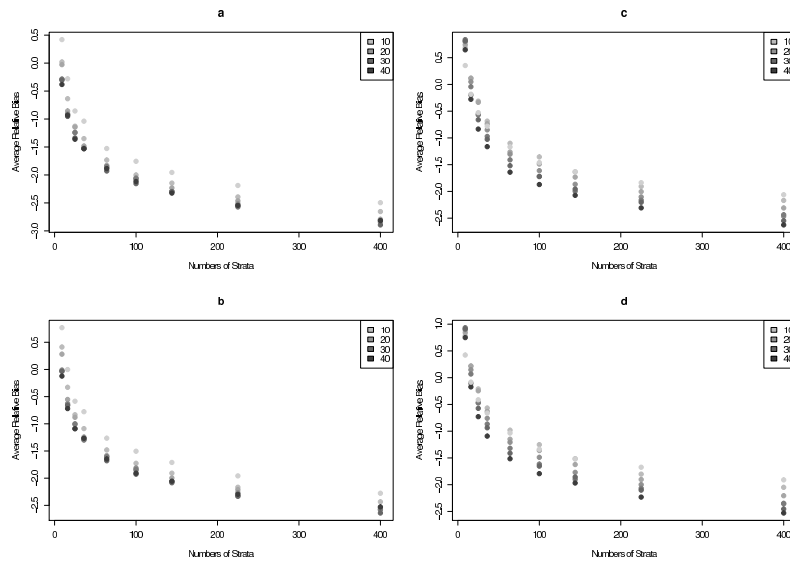


Figure 15: Urchins : Average relative bias in log scale depending on the number of strata and the number of measure points.

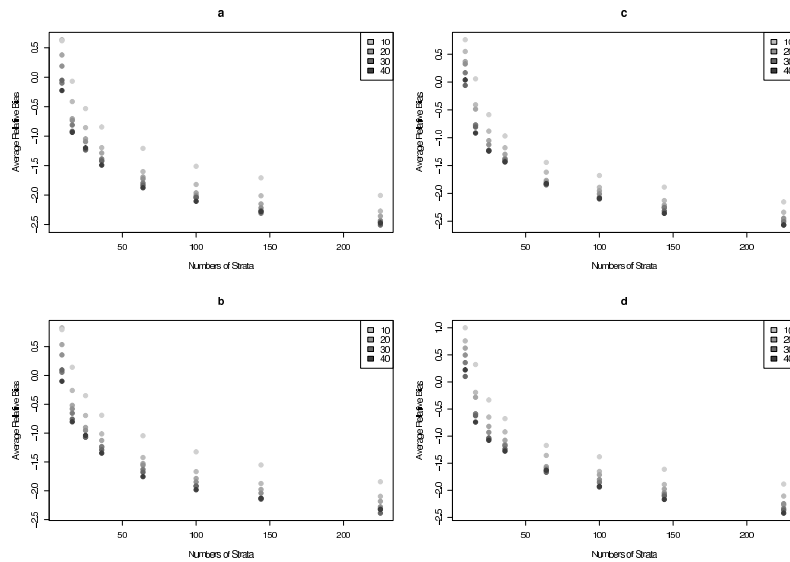


Figure 16: Starfish : Average relative bias in log scale depending on the number of strata and the number os measure points.

383 fulfilled and the design of the case study seems acceptable. For  $\theta^{Urchin}$  however,  
 384 the present design should be strongly re-enforced (up to 40 points per stratum  
 385 with 36 strata!) before yielding acceptable estimations, and confidence regions  
 386 based on asymptotical theory are definitely too optimistic.

387 These two sets of parameter recover two very different situations : the larger



388 number of zeros in the Urchin case may render the estimation procedure more  
 389 difficult than in the Starfish situation. However one should note that the difference  
 390 is not markedly pronounced : 34% instead of 24%! Such a simulation study  
 391 shows that the quality of variance covariance matrix estimation used to build an  
 392 ellipsoid of confidence behaves has to be checked through this simulation approach  
 393 by instance to verify whether the asymptotic conditions are fulfilled and that the  
 394 analyst should beware of overconfidence.

Urchin-like

| N strata | Number of points per stratum (M) |       |      |      |      |      |      |
|----------|----------------------------------|-------|------|------|------|------|------|
|          | 5                                | 10    | 15   | 20   | 25   | 30   | 40   |
| S        | 54.5                             | 56.9  | 61.3 | 65   | 66.4 | 68.5 | 75.2 |
| 9        | 54.5                             | 56.9  | 61.3 | 65   | 66.4 | 68.5 | 75.2 |
| 16       | 56                               | 60.3  | 64.6 | 69.5 | 73.8 | 78.5 | 82.3 |
| 25       | 58.45                            | 62.45 | 66.8 | 75   | 75   | 83   | 86.6 |
| 36       | 55.8                             | 65.2  | 71.9 | 75   | 80.4 | 83.3 | 89.2 |
| 64       | 60.8                             | 64.3  | 74.8 | 78.3 | 84.7 | 85.7 | 88.9 |
| 100      | 59                               | 66.3  | 74.4 | 79.2 | 86.3 | 85.5 | 90   |
| 144      | 57.3                             | 68.2  | 75.6 | 83.1 | 86.7 | 86   | 91   |
| 225      | 55.1                             | 68.9  | 74.8 | 75   | 84.6 | 86.2 | 89.5 |
| 400      | 51.7                             | 68.9  | 78   | 83.2 | 83.9 | 88   | 88.9 |

Urchin-like

| N strata | Number of points per stratum (M) |      |      |      |      |      |      |
|----------|----------------------------------|------|------|------|------|------|------|
|          | 5                                | 10   | 15   | 20   | 25   | 30   | 40   |
| S        | 63.8                             | 78.9 | 79.7 | 86.2 | 88.1 | 89.3 | 89.3 |
| 9        | 63.8                             | 78.9 | 79.7 | 86.2 | 88.1 | 89.3 | 89.3 |
| 16       | 70.7                             | 84.6 | 87.9 | 88.6 | 89.5 | 91.3 | 91.7 |
| 25       | 78.5                             | 87.8 | 89   | 91.5 | 90.6 | 92.4 | 91.9 |
| 36       | 84.4                             | 87.2 | 86.7 | 88.7 | 89.7 | 92.2 | 92.2 |
| 64       | 87                               | 89.6 | 89.6 | 88.8 | 90.5 | 92.1 | 91.2 |
| 100      | 88                               | 89.5 | 89.4 | 90.9 | 91.3 | 92.5 | 91.4 |
| 144      | 86.6                             | 85.9 | 90.7 | 90.9 | 90.1 | 89.9 | 90   |
| 225      | 89.3                             | 90.7 | 88.9 | 90   | 90.5 | 91.5 | 92   |
| 400      | 89.9                             | 89.8 | 91.3 | 90.3 | 88.7 | 92.1 | 89   |

Figure 17: Urchin-like case. Effective proportion of 90% confidence intervals that cover the true value. Shading in particular cells reflects the degree of overlap: M-S combination that produces confidence intervals that are too liberal are in black whereas the lightest grey shade reflects confidence intervals that properly characterize parameter uncertainty

Figure 18: Sunstar-like case. Effective proportion of 90% confidence intervals that cover the true value. Shading in particular cells reflects the degree of overlap: M-S combination that produces confidence intervals that are too liberal are in black whereas the lightest grey shade reflects confidence intervals that properly characterize parameter uncertainty.

## 395 5. Conclusion and Perspectives

396 The following conclusions have been reached:

- 397 1. Compound Poisson distributions can conveniently represent the presence of  
 398 a large number of zeros and a skewed distribution of non-zero values. To  
 399 deal the occurrence of zero-inflated data, very parsimonious models can be  
 400 designed (with two parameters only) : a Poisson random sum of independent  
 401 geometric random variables in the discrete case and with exponential random  
 402 variables in the continuous one. They offer an alternative to the traditionnal

403 delta gamma models and behave coherently when changing the scale of the  
404 catch effort, thanks to the Poisson process underpinning the model.

405 2. Compound Poisson distributions can be interpreted using a hierarchical frame-  
406 work. They describe the data collection involved in sampling individuals  
407 gathered in (latent) patches drawn from the homogeneous Poisson process  
408 with *abundance* tuned by the distributional parameter of the random com-  
409 ponents of the Poisson sum. The introduction of a random effect structure  
410 at the top of the hierarchy is straightforward and accommodates non homo-  
411 geneity among strata that are themselves considered as homogeneous units.  
412 Such designs with random effects and data with extra zeros are commonly  
413 encountered in ecological analyzes, but gamma random effects are yet rarely  
414 advocated : variation between strata is typically modeled using a normal (or  
415 lognormal) distribution because its sufficient statistics match the common-  
416 sense interpretation of mean and variance. However, gamma random effects  
417 allow for partial conjugate properties with the compound Poisson model for  
418 zero-inflated data. Beyond this theoretical convenience, the parameters of  
419 the gamma distribution are well estimated in the Starfish like simulation  
420 examples and they can describe the entire range of variability between units  
421 for the real case study.

422 3. Independence between the latent features  $\rho$  and  $\mu$  has been a priori assumed  
423 for the random effects between units. This absence of prior correlation is  
424 quite a stringent hypothesis as we might expect  $\rho$  and  $\mu$  to covary (e.g, low  
425 non-zero realized abundance could stem from either a small  $\mu$  or a large  
426  $\rho$ ). Working with a gaussian copula for a joint bivariate distribution for  
427 the couple  $(\mu, \rho)$  is a bad remedy, because we would have lost the conjugate  
428 properties and increased computational load. To keep partial conjugacy , a  
429 better idea is considering the natural extension of the gamma family, but  
430 such bivariate distributions are rather restrictive since they can only take  
431 into account positive correlation and need that the two marginals share the  
432 same shape parameter. However such a model would remain parsimonious  
433 with 4 parameters: one is gained to depict correlation and one is lost to  
434 depict the marginals' shape. The issue of correlation has been addressed in  
435 [2] who proved via simulation that the correlation between  $\rho$  and  $\mu$  has little  
436 bearing on the property we are ultimately trying to predict in practice, i.e.  
437 the realized biomass in a tow. Finally, the correlation indicates that the  
438 latent variables  $\rho$  and  $\mu$  are model concepts that should themselves not be  
439 overinterpreted; they don't actually characterize the true size and number of  
440 organism patches.

441 4. Stochastic EM inferential techniques (with importance sampling for the non

442 explicit expectation steps) require a modest computational effort since the  
443 random effects are taken partially conjugate with the compound Poisson  
444 distributions. Auxiliary importance distributions can be proposed by careful  
445 inspection the structure of the joint distribution of the latent variables and  
446 integrating out as much as can analytically be done. Much advantage is  
447 taken from conditional independence, especially when computing the Fisher  
448 information matrix by re-sampling with the simulated missing data that  
449 have been previously generated to evaluate the maximum likelihood estimate.  
450 However, the value of results given here depends on the errors involved with  
451 the use of maximum likelihood asymptotic formula on one hand and on  
452 the precision of Monte Carlo sampling algorithms on the other hand. Due  
453 to the multidimensional nature of the latent variables to be simulated , the  
454 variability between several trials of the importance sampling techniques when  
455 evaluating the information matrix (and its inverse) can be important enough,  
456 especially when few data makes a rather flat likelihood function.

- 457 5. Asymptotic errors bounds need to be checked and corrected if necessary. We  
458 relied on a simulation study to get a more reliable idea of their ranges. The  
459 simulated sets of zero-inflated data show that, in the Starfish case, one can  
460 readily trust the confidence intervals based on the information matrix while  
461 in the Urchin case, one should beware of being overconfident. The asymp-  
462 totic conditions may not be encountered rapidly. For the Starfish case study,  
463 the design allowed a reasonable estimation of the RLOL model features. For  
464 the other species with a 10% higher probability of getting zero values, satisf-  
465 ying precision estimates with 40 strata need at least collecting 40 data points  
466 per stratum before the confidence coverage gets reasonably close to its theo-  
467 retically recommended approximate value. Because 1600 stations represents  
468 generally unrealistically large sampling effort for a marine bottom-trawl sur-  
469 vey in that Urchin example, statisticians need to inform practitioners (before  
470 launching the data collection) about possible underestimation of uncertainty.
- 471 6. Covariates for the fixed effect of environmental variable (depth, temperature  
472 and habitat type) could be added to the model, potentially enhancing eco-  
473 logical interpretation of the observed patterns in organism abundance and  
474 distribution. However, it may bring a lot of additional burden during the in-  
475 ferential computations since many of the conjugate properties would be lost.  
476 For the same reasons, non exchangeable strata (with for instance an intrinsic  
477 CAR structure on the top of the hierarchy as described in (author?) [3])  
478 have not been considered here. Simple (low dimensional) importance sam-  
479 pling should be replaced with brute force Hastings Metropolis techniques  
480 [11]. In such a context, it may be worthwhile to work on encoding prior

481 knowledge [14] into probability distributions and switch the problem into a  
482 Bayesian framework [5], relying on ready-made tools such as WinBugs for  
483 inference [24].

484 7. In the case study, the random effect models with compound Poisson distri-  
485 bution for the occurrence of zero-inflated data fit the data well and allow  
486 transfer of information between strata to help predict in data-poor units. Its  
487 hierarchical structure favors discussion between ecologists and statisticians,  
488 and helps query its interpretation in term of ecological situations with extra  
489 zeros.

## 490 References

- 491 [1] M. Abramowitz and I.A. Stegun. *Handbook of Mathematical Functions with*  
492 *Formulas, Graphs and Mathematical Tables*. Chapman & Hall, 2004.
- 493 [2] Sophie Ancelet. *Exploiter l'approche hiérarchique bayésienne pour la*  
494 *modélisation statistique de structures spatiales*. PhD thesis, UMR 518  
495 AgroParisTech/INRA Mathématiques et Informatique Appliquées, F-75231  
496 Paris, France, 2008.
- 497 [3] Sudipto. Banerjee, Bradley P. Carlin, and Alan E. Gelfand. *Hierarchical*  
498 *Modeling and analysis for spatial data*. Wiley, 2004.
- 499 [4] S.C. Barry and A.H. Welsh. Generalized additive modelling and zero inflated  
500 count data. *Ecological Modelling*, 157:179–188, 2002.
- 501 [5] J. O. Berger. *Statistical Decision Theory and Bayesian Analysis*. Springer-  
502 Verlag, New York, 1985.
- 503 [6] J. Bernier and D. Fandoux. Théorie du renouvellement - application à l'étude  
504 statistique des précipitations mensuelles. *Revue de Statistique Appliquée*,  
505 XVIII(2):75–87, 1970.
- 506 [7] A. Dempster, N. Laird, and D. Rubin. Maximum likelihood from incomplete  
507 data via the EM algorithm. *Jour. Roy. Statist. Soc.*, 40:1–22, 1978.
- 508 [8] B. Delyon, M. Lavielle, and E. Moulines. Convergence of a stochastic approx-  
509 imation version of EM algorithm. *Ann. Statist.*, 27:94–128, 1999.
- 510 [9] W. Feller. *An Introduction to Probability Theory and Its Applications*, vol-  
511 ume 2. Wiley, second edition, 1971.

- 512 [10] A.E. Gelfand and A.F.M. Smith. Sampling based approach to calculating  
513 marginal densities. *Journal of the American Statistical Association*, 85:398–  
514 409, 1990.
- 515 [11] W.K. Hastings. Monte Carlo sampling methods using markov chains and their  
516 applications. *Biometrika*, 57:97–109, 1970.
- 517 [12] D.C Heilbron. Zero-altered and other regression models for count data with  
518 added zeros. *Biometrical Journal*, 36:531–547, 1994.
- 519 [13] Tim C. Hesterberg. Unbiasing the bootstrap-bootknife sampling vs. smooth-  
520 ing. *Proceedings of the Section on Statistics and the Environment*, pages  
521 2924–2930, 2004.
- 522 [14] J.B. Kadane, L.J. Wolson, A. O’Hagan, and K. Craig. Papers on elicitation  
523 with discussions. *The Statistician*, pages 3–53, 1998.
- 524 [15] A. Richard Levine and George Casella. Implementations of the Monte Carlo  
525 EM algorithm. *Journal of Computational and Graphical Statistics*, 10(3):422–  
526 439, 2001.
- 527 [16] B.A. Martin, T.G. and Wintle, J.R. Rhodes, P.M. Kuhnert, S.A. Field, S.J.  
528 Low-Choy, A.J. Tyre, and H.P. Possingham. Zero tolerance ecology: improv-  
529 ing ecological inference by modelling the source of zero observations. *Ecology*  
530 *Letters*, 8:1235–1246, 2005.
- 531 [17] P. McCullagh and J. A. Nelder. *Generalized Linear Models*. Chapman & Hall,  
532 1983.
- 533 [18] C. E. McCulloch. Maximum likelihood variance components estimation for  
534 binary data. *Journal of the American Statistical Association*, 1994.
- 535 [19] C. E. McCulloch. Maximum likelihood algorithms for generalized linear mixed  
536 models. *Journal of the American Statistical Association*, 1997.
- 537 [20] M.K Pitt and N. Shephard. Filtering via simulation : auxiliary particle filters.  
538 *Journal of the American Statistical Association*, 94:590–599, 1999.
- 539 [21] M. Ridout, C. Demetrio, and J. Hinde. Models for count data with many  
540 zeros. *International Biometric Conference*, pages 1–13, 1998.
- 541 [22] C.P. Robert and G. Casella. *Monte Carlo Statistical Methods*. Springer-Verlag,  
542 1998.

- 543 [23] D.J. Spiegelhalter, A. Thomas, and N.G. Best. Computation on Bayesian  
544 graphical models (avec discussion). In J.M. Bernardo, J.O. Berger, A.P.  
545 Dawid, and A.F.M. Smith, editors, *Bayesian Statistics*, pages 407–425.  
546 Clarendon Press, 1996.
- 547 [24] D.J. Spiegelhalter, A. Thomas, and N.G. Best. *WinBUGS Version 1.3. User*  
548 *Manual*. MRC Biostatistics Unit, 2000.
- 549 [25] G. Stefansson. Analysis of groundfish survey abundance data: combining  
550 the glm and delta approaches. *ICES Journal of Marine Science*, 53:577–588,  
551 1996.
- 552 [26] S.E. Syrjala. Critique on the use of the delta distribution for the analysis of  
553 trawl survey data. *ICES Journal of Marine Science*, 57:831–842, 2000.
- 554 [27] M. H. Tanner. *Tools for Statistical Inference : Observed Data and Data*  
555 *Augmentation Methods*. Springer-Verlag, New York, 1992.
- 556 [28] Martin Abba Tanner. *Tools for statistical inference: Methods for the ex-*  
557 *ploration of posterior distributions and likelihood functions*. Springer-Verlag,  
558 New York, 1996.
- 559 [29] K. W. Wickle, L. M. Berliner, and N. Cressie. Hierarchical Bayesian space-  
560 time models. *Environmental and Ecological Statistics*, 5:117–154, 1998.

561 APPENDICES

562 **A. Compound Poisson process characteristic function**

When  $X$  is real valued, we denote by  $\hat{f}$  the Fourier transform<sup>1</sup> of  $f$  (i.e the characteristic function of  $X$ ) :

$$\hat{f}(\omega) = E(e^{i\omega X})$$

From equation 2.1, the compound Poisson distribution  $g$  is such that :

$$\hat{g}(\omega) = \sum_{n=0}^{\infty} e^{-\mu} \frac{\mu^n}{n!} \left( \hat{f}(\omega) \right)^n = e^{-\mu(1-\hat{f}(\omega))} \quad (\text{A.1})$$

---

<sup>1</sup>For non negative integer valued random variables  $X$  the probability generating function  $P(z) = \sum_0^{\infty} \Pr(X = n)z^n$  is the corresponding machinery for handling discrete distributions : the same results can be found in this case by setting the change of variables  $z = e^{i\omega}$

563 This equation exhibits the infinite divisibility property of  $Y$  with regards to  
564 parameter  $\mu$ , which offers a nice conceptual interpretation when returning to the  
565 marked Poisson process underneath this stochastic construction : the resulting  
566 quantity  $Y$  is obtained by collecting a random number of primarily (hidden)  
567 batches  $X_i$  distributed at random with intensity  $\mu$ . Such a conceptual latent  
568 process of aggregates would be intuitive for many ecologists. Conversely, one can  
569 easily check by writing the logarithm of their characteristic functions, that tradi-  
570 tional models for zero-inflated data (think for instance of the delta-gamma model  
571 or the Zero-Inflated Poisson model such as [21]) lack of coherence for adapting to  
572 a change of the scale in the experiment.

Among the many choices for the probability distribution  $f$  of the random mark  
of the sum, this paper focuses, for parsimony and realism, on the exponential  
distribution for  $X$  (continuous case) that is :

$$f(x) = \rho e^{-\rho x}$$

573 so that  $\hat{f}(\omega) = \frac{\rho}{\rho+i\omega}$  and  $\hat{g}(\omega) = e^{-\mu(\frac{i\omega}{\rho+i\omega})}$ . For the discrete case, we suggest  
574 the corresponding geometric distribution :  $f(x) = 1_{x>0} \times (1-r) \times r^x e^{i\omega x}$  leading  
575 to  $\hat{f}(\omega) = \frac{1-r}{1-re^{i\omega}}$  and  $\hat{g}(\omega) = e^{-\mu(\frac{r(1-e^{i\omega})}{1-re^{i\omega}})}$  for the exponential compound Poisson  
576 count model.

## 577 B. Initialization of the Newton-Raphson algorithm

The main point on Newton-Raphson algorithm consists in choosing a good  
initial point. In this paper we use this algorithm to find the zero of

$$\ln(a) - \psi(a) - C = 0$$

Note that function  $\psi$  verifies the following asymptotic series' expansion [1] :

$$\begin{aligned} \psi(x) &\underset{x \rightarrow \infty}{\sim} \ln(x) - \frac{1}{2x} - \sum_{n=1}^{\infty} \frac{B_{2n}}{2n x^{2n}} \\ &\underset{x \rightarrow \infty}{\sim} \ln(x) - \frac{1}{2x} - \frac{1}{12 x^2} + \frac{1}{120 x^4} + \dots \end{aligned}$$

578 The convergence is very fast (see Figure 19) so that we choose to initiate Newton-  
579 Raphson algorithm with  $x_0 = \frac{1}{2C}$ .

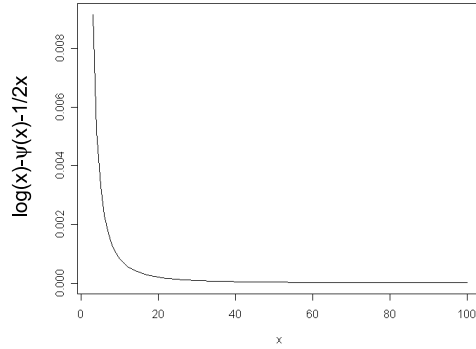


Figure 19: Difference between  $\log(x) - \psi(x)$  and  $1/2x$

580 **C. Computation of the moments of gamma and log gamma, beta and**  
 581 **log beta distribution implied in the expectation step**

582 *C.1. First and second moments for the sufficient statistics of the gamma pdf*

Let  $Z$  be a random variable with gamma distribution,  $Z \sim \Gamma(s, t)$ . Using laplace transform it is easy to obtain the first moment of  $\ln(Z)$  :

$$\mathbb{E}(e^{\lambda \ln(Z)}) = \mathbb{E}(Z^\lambda) = \frac{t^s}{\Gamma(s)} \int_0^{+\infty} y^\lambda y^{s-1} e^{-ty} dy = \frac{\Gamma(s + \lambda)}{\Gamma(s)t^\lambda}.$$

Differentiating this equation with respect to  $\lambda$ , we have the expected value of  $\ln(Z)$  (when  $\lambda = 0$ ) and  $Z \ln(Z)$  (when  $\lambda = 1$ ):

$$\left. \frac{\partial \mathbb{E}(Z^\lambda)}{\partial \lambda} \right|_{\lambda=0} = \mathbb{E}(\ln(Z)) = \psi(s) - \ln(t), \quad (\text{C.1})$$

and

$$\left. \frac{\partial \mathbb{E}(Z^\lambda)}{\partial \lambda} \right|_{\lambda=1} = \mathbb{E}(Z \ln(Z)) = \frac{s}{t} (\psi(s + 1) - \ln(t)). \quad (\text{C.2})$$

583 Taking the second order derivative, we show :

$$\left. \frac{\partial^2 \mathbb{E}(Z^\lambda)}{\partial \lambda^2} \right|_{\lambda=0} = \mathbb{E}(\ln(Z)^2) = \psi'(s) + \psi(s)^2 - 2 \ln(t)\psi(s) + \ln(t)^2. \quad (\text{C.3})$$



Therefore the variance-covariance matrix between  $Z$  and  $\ln(Z)$  is :

$$\begin{pmatrix} \frac{s}{t^2} & \frac{1}{t} \\ \frac{1}{t} & \psi'(s) \end{pmatrix}$$

584 *C.2. First and second moments for the sufficient statistics of the beta pdf*

Let  $S$  be a random variable with beta distribution  $S \sim \beta(s, t)$ .

$$\mathbb{E}(e^{\lambda \ln(S)}) = \frac{\Gamma(s+t) \Gamma(s+\lambda)}{\Gamma(s+t+\lambda) \Gamma(s)}$$

So that, by first and second differentiation, one gets, (the derivation is quite straightfully performed if working with  $\ln \mathbb{E}(e^{\lambda \ln(S)})$ ) :

$$\begin{aligned} \mathbb{E}(\ln(S)) &= \psi(s) - \psi(s+t) \quad , \quad \mathbb{E}(\ln(1-S)) = \psi(t) - \psi(s+t) \\ \mathbb{E}(\ln(S)^2) &= \psi'(s) - \psi'(s+t) + (\psi(s) - \psi(s+t))^2 \end{aligned}$$

One can extend the properties of characteristic function by considering the function of the two arguments  $\lambda$  and  $\mu$

$$\mathbb{E}(e^{\lambda \ln(S) + \mu \ln(1-S)}) = \frac{\Gamma(s+t) \Gamma(s+\lambda) \Gamma(t+\mu)}{\Gamma(s+t+\lambda) \Gamma(s) \Gamma(t)}$$

585 By cross-differentiation under regularity conditions (working with  $\ln \mathbb{E}(S^\lambda(1-S)^\mu)$   
586 makes things easier here also) , the joint moment can be analytically obtained :

$$\begin{aligned} \left. \frac{\partial^2 \mathbb{E}(S^\lambda(1-S)^\mu)}{\partial \lambda \partial \mu} \right|_{\lambda=0, \mu=0} &= \mathbb{E}(\ln(S) \ln(1-S)) \\ &= -\psi'(s+t) + \mathbb{E}(\ln(S)) \mathbb{E}(\ln(1-S)) \end{aligned}$$

Therefore the variance-covariance matrix between  $\ln(S)$  and  $\ln(1-S)$  reads :

$$\begin{pmatrix} \psi'(s) - \psi'(s+t) & -\psi'(s+t) \\ -\psi'(s+t) & \psi'(t) - \psi'(s+t) \end{pmatrix}$$

## 587 D. EM algorithm principle

From a constructive point of view, one often writes

$$[x, z | \theta] = [x | \theta, z] \times [z | \theta],$$

but using Bayes rule, we may write the reverse logarithmic form :

$$\ln [x | \theta] = \ln [x, z | \theta] - \ln [z | \theta, x] \quad (\text{D.1})$$

588 Let us remark that relation D.1 is valid whatever  $z$  represents.

589 *D.1. Recall about EM algorithm and control of the gradient*

Under regularity conditions for the joint distribution  $[x, z | \theta]$  and the conditional one  $[z | \theta, x]$ , integrating relation D.1 with respect to the probability density  $[z | \theta', x]$  :

$$\begin{aligned} \ln [x | \theta] &= \int_z \ln [x, z | \theta] [z | \theta', x] dz - \int_z \ln [z | \theta, x] [z | \theta', x] dz \\ &= Q(\theta, \theta') - H(\theta, \theta') \end{aligned} \quad (\text{D.2})$$

590 The maximum of  $\theta \mapsto H(\theta, \theta')$  is achieved in  $\theta = \theta'$  [27].  
So  $H(\theta, \theta') < H(\theta', \theta')$ . Let us consider D.2 for  $\theta$  and  $\theta'$

$$\ln [x | \theta] - \ln [x | \theta'] = (Q(\theta, \theta') - Q(\theta', \theta')) + (H(\theta', \theta') - H(\theta, \theta'))$$

EM algorithm is based upon an iterative procedure which exhibits  $\theta$  such that  $Q(\theta, \theta') > Q(\theta', \theta')$ . The best  $\theta$  is obtained by

$$\theta = \underset{\theta}{\operatorname{argmax}} Q(\theta, \theta')$$

During iteration we can monitor the value of the gradient for the log likelihood :

$$\frac{\partial \ln [x | \theta]}{\partial \theta} = \frac{\partial \ln [x, z | \theta]}{\partial \theta} - \frac{\partial \ln [z | \theta, x]}{\partial \theta} \quad (\text{D.3})$$

Integrating the right hand term with respect to conditional density  $[z | \theta, x]$ , and keeping in mind that, for any sufficiently regular *pdf*  $f(z; \theta)$  of variable  $z$  with parameter  $\theta$  one can write:  $\int_z \frac{\partial \ln f(z, \theta)}{\partial \theta} f(z; \theta) dz = \frac{\partial}{\partial \theta} \int_z \frac{\partial \ln f(z, \theta)}{\partial \theta} f(z; \theta) dz = 0$ , we

have

$$\begin{aligned} \frac{\partial \ln [x | \theta]}{\partial \theta} &= \int_z \frac{\partial \ln [x, z | \theta]}{\partial \theta} [z | \theta, x] dz - \int_z \frac{\partial \ln [z | \theta, x]}{\partial \theta} [z | \theta, x] dz \\ \frac{\partial \ln [x | \theta]}{\partial \theta} &= \int_z \frac{\partial \ln [x, z | \theta]}{\partial \theta} [z | \theta, x] dz \end{aligned} \quad (\text{D.4})$$

591 We may use this equality (computed by Monte Carlo method) to perform a  
 592 gradient method to obtain the maximum likelihood or just to check along the  
 593 iterations that the gradient is going to zero.

594 *D.2. Score function*

From now on, let's call  $Sc(\theta, z, x) = \frac{\partial \ln[x, z | \theta]}{\partial \theta}$  the score, i.e the complete loglike-  
 likelihood gradient and  $Sc(\theta_i, z, x) = \frac{\partial \ln[x, z | \theta]}{\partial \theta_i}$  its  $i^{th}$  component.  $\nabla \theta$ , equation D.4  
 proves that its conditional expectation (with respect to  $[z | \theta, x]$ ) is always equal to  
 the likelihood gradient. Pushing the derivation game one step further leads to:

$$\begin{aligned} \frac{\partial}{\partial \theta_j} \left\{ \frac{\partial \ln [x | \theta]}{\partial \theta_i} \right\} &= \int_z \left\{ \frac{\partial Sc_i}{\partial \theta_j} [z | \theta, x] + Sc_i \frac{\partial [z | \theta, x] [z | \theta, x]}{\partial \theta_j [z | \theta, x]} \right\} dz \\ \frac{\partial^2 \ln [x | \theta]}{\partial \theta_i \partial \theta_j} &= \int_z \left\{ \frac{\partial^2 \ln [x, z | \theta]}{\partial \theta_i \partial \theta_j} + Sc_i \left( Sc_j - \frac{\partial \ln [x | \theta]}{\partial \theta_j} \right) \right\} [z | \theta, x] dz \end{aligned} \quad (D.5)$$

595 *D.3. Information matrix*

To obtain the covariance matrix of the estimators at the maximum of likeli-  
 hood, the empirical information matrix needs to be computed. The second order  
 derivative is obtained by differentiating D.1:

$$\frac{\partial^2 \ln [x | \theta]}{\partial \theta_i \partial \theta_j} = \frac{\partial^2 \ln [x, z | \theta]}{\partial \theta_i \partial \theta_j} - \frac{\partial^2 \ln [z | \theta, x]}{\partial \theta_i \partial \theta_j} \quad (D.6)$$

At the maximum  $\theta = \hat{\theta}$ , formula D.3 implies  $\frac{\partial \ln[x | \theta]}{\partial \theta_{jj}} = 0$  so that equation D.5  
 takes a more friendly aspect because the score term  $\frac{\partial \ln[x | \theta]}{\partial \theta_j}$  in the right hand side  
 vanishes at  $\theta = \hat{\theta}$ . Equation D.6 becomes therefore much more handy because  
 it only involves conditional expectations of first and second derivatives of the  
 complete likelihood terms :

$$\frac{\partial^2 \ln([x | \hat{\theta}])}{\partial \theta_i \partial \theta_j} = \int_z \left( \frac{\partial^2 \ln [x, z | \hat{\theta}]}{\partial \theta_i \partial \theta_j} + \frac{\partial \ln [x, z | \hat{\theta}]}{\partial \theta_i} \frac{\partial \ln [x, z | \hat{\theta}]}{\partial \theta_j} \right) [z | \hat{\theta}, x] dz \quad (D.7)$$

596 As  $\int_z \left( \frac{\partial \ln [x, z | \hat{\theta}]}{\partial \theta_j} \right) [z | \hat{\theta}, x] dz = \frac{\partial \ln [x | \hat{\theta}]}{\partial \theta_j} = 0$ , the second term in the right hand  
 597 side of eq D.7 can be considered as the conditional variance of the gradient of the

598 complete log-likelihood  $\ln [x, z | \hat{\theta}]$ . This expectation can be numerically com-  
 599 puted with the same techniques to which recourse was made for the EM algorithm.

## 600 E. Detailed proofs of propositions

### 601 E.1. Proof of proposition 3.1

Since we detail the computation for one particular  $s$ , we will omit to mention it in order to make the reading easier. We also note respectively  $\underline{y}$ ,  $\underline{D}$  and  $\underline{N}$  the vectors of data, catching efforts and corresponding number of clumps in one stratum.

We define  $J$  as

$$J(\underline{N}, \rho, \mu) = [\rho, \mu, \underline{N} | a, b, c, d, \underline{y}, \underline{D}]. \quad (\text{E.1})$$

Then  $J$  satisfies the following set of equations :

$$\begin{aligned} &\propto [\underline{y}, \rho, \mu, \underline{N} | a, b, c, d, \underline{D}] \\ &\propto \left( \prod_{i=1}^I [y_i | N_i, \rho] [N_i | \mu, D_i] \right) [\mu | a, b] [\rho | c, d] \\ &\propto \left( \prod_{i=1}^I [y_i | N_i, \rho, \mu] [N_i | \rho, \mu] \right) (\mu^{a-1} e^{-\mu b}) (\rho^{c-1} e^{-\rho d}) \end{aligned}$$

with the convention that  $[A|B] \propto f(A, B)$  means that the coefficient of proportionality only depends on  $B$ . We note  $I^*$  the number of zero value  $y$  and we reorder the vector  $y$  so that the  $I^+ = I - I^*$  non zero  $y_i$  are the first, so that  $J$  may be written as :

$$\begin{aligned} J(\underline{N}, \rho, \mu) &\propto \left( \prod_{i=1}^{I-I^*} \left( \frac{y_i^{N_i} e^{-\rho y_i} \rho^{N_i}}{\Gamma(N_i)} \right) \left( \frac{e^{-\mu D_i} (\mu D_i)^{N_i}}{\Gamma(N_i + 1)} \right) \right) \\ &\quad \left( \prod_{i^*=I-I^*+1}^I \delta(N_{i^*}) e^{-\mu D_{i^*}} \right) (\mu^{a-1} e^{-\mu b}) (\rho^{c-1} e^{-\rho d}) \end{aligned}$$

Defining  $Y_+ = \sum_{i=1}^I y_i$ ,  $N_+ = \sum_{i=1}^I N_i$  and  $D_+ = \sum_{i=1}^I D_i$ , we obtain :

$$J(\underline{N}, \rho, \mu) \propto \left( \prod_{i=1}^{I^+} \frac{y_i^{N_i}}{\Gamma(N_i) \Gamma(N_i + 1)} \right) e^{-\rho(Y_+ + d)} \rho^{N_+ + c - 1} e^{-\mu(D_+ + b)} \mu^{N_+ + a - 1}$$

Conditionally to the latent vector  $\underline{N}$ , the random effects  $\rho$  and  $\mu$  are independent. Isolating the terms which depend on  $\mu$  on one side and those depend on  $\rho$  on the

other, we find that

$$\begin{aligned} [\mu | \underline{N}, \theta, \underline{y}, \underline{D}] &\sim \Gamma(a + N_+, b + D_+) \\ [\rho | \underline{N}, \theta, \underline{y}] &\sim \Gamma(c + N_+, d + Y_+) \end{aligned}$$

For the expectation step we only need to compute  $\mathbb{E}_\theta(\mu_s | Y_s)$ ,  $\mathbb{E}_\theta(\ln(\mu_s) | Y_s)$  and the same sufficient statistics concerning  $\rho$ .

Since  $\mu_s | \underline{N}_s, \theta, \underline{y}$  follows a gamma distribution  $\Gamma(a + N_{s+}, b + D_{s+})$ , the conditional expected value  $\mu_s$  given  $\underline{N}_s$  and  $\theta = (a, b, c, d)$  is  $(a + N_{s+}) / (b + D_{s+})$ .

Then

$$\mathbb{E}_{\theta'}(\mu_s | \underline{y}_s) = \mathbb{E}_{\theta'}\left(\frac{a' + N_{s+}}{b' + D_{s+}} | \underline{y}_s\right) = \frac{a' + \mathbb{E}_{\theta'}(N_{s+} | \underline{y}_s)}{b' + D_{s+}}.$$

If  $Z$  follows gamma distribution  $\Gamma(s, t)$ , then  $\mathbb{E}(\ln(Z)) = \psi(s) - \ln(t)$  (see annex C), so that

$$\mathbb{E}_{\theta'}(\ln(\mu_s) | \underline{y}_s) = \mathbb{E}_{\theta'}(\psi(a' + N_{s+}) | \underline{y}_s) - \ln(b' + D_{s+}).$$

We have respectively for  $\rho_s$

$$\mathbb{E}_{\theta'}(\rho_s | \underline{y}_s) = \frac{c' + \mathbb{E}_{\theta'}(N_{s+} | \underline{y}_s)}{d' + Y_{s+}},$$

and

$$\mathbb{E}_{\theta'}(\ln(\rho_s) | \underline{y}_s) = \mathbb{E}_{\theta'}(\psi(c' + N_{s+}) | \underline{y}_s) - \ln(d' + Y_{s+}).$$

## 602 E.2. Proof of proposition 3.2

603 Let us define  $J$  as the distribution of  $[\rho, \mu, \underline{N} | \theta', \underline{y}, \underline{D}]$  in one particular stratum  
 604  $s$ . We will write  $J$  in a bottom-up perspective and consider the distribution of  $\mu$   
 605 and  $\rho$  conditioned by  $N$ , because  $\mu$  and  $\rho$  are conditionally independant.

$J$  is given by :

$$\begin{aligned} J(\underline{N}, \rho, \mu) &= [\rho, \mu, \underline{N} | \theta', \underline{y}, \underline{D}] \\ &= [\rho | \underline{N}, \theta, \underline{y}] [\mu | \underline{N}, \theta', \underline{y}, \underline{D}] [\underline{N} | \theta, \underline{y}, \underline{D}] \end{aligned}$$

Using the independent conditional gamma distributions of  $\mu$  and  $\rho$  and integrating according to  $\mu$  and  $\rho$  given  $\underline{N}$ , we can exhibit all the terms depending on

$\underline{N}$ .

$$\int_{\rho} \int_{\mu} J(\underline{N}, \rho, \mu) d\mu d\rho = [\underline{N} | \theta, \underline{y}, \underline{D}]$$

$$\propto \prod_{i=1}^{I^+} \left( \frac{y_i^{N_i}}{\Gamma(N_i)\Gamma(N_i+1)} \right) \prod_{i^*=I-I^*+1}^I \delta(N_{i^*}) \left( \frac{(b' + D_+)^{N_+} (d + Y_+)^{N_+}}{\Gamma(a + N_+)\Gamma(c + N_+)} \right)^{-1}$$

606 *E.3. Proof of proposition 3.4*

In the following  $Z$  will stand for all the hidden variables i.e  $\underline{Z} = (\underline{N}, \underline{\mu}, \underline{\rho})$ ,  $|M_{ij}|$  is another notation for matrix  $M$  that details the content of the  $i^{th}$  row and  $j^{th}$  column, and  $\frac{\partial F(\theta)}{\partial \theta}$  stands for the gradient of  $F$  written as a vector whose  $i^{th}$  component is the scalar  $\frac{\partial F(\theta)}{\partial \theta_i}$ . The key equation involves rewriting equation D.7 as the expectation of the second order derivative of the complete log-likelihood and the variance of the score (its gradient) to be taken with regards to the conditional distribution  $[Z | x, \hat{\theta}]$  (see annex D.3)

$$\left| \frac{\partial^2 \ln([x | \hat{\theta}])}{\partial \theta_i \partial \theta_j} \right| = \mathbb{E}_{Z|x} \left| \frac{\partial^2 \ln([x, Z | \hat{\theta}])}{\partial \theta_i \partial \theta_j} \right| + \text{Var}_{Z|x} \left( \frac{\partial \ln [x, Z | \theta]}{\partial \theta} \right) \quad (\text{E.2})$$

Computing the first term of the right hand side of equation E.2 is easy, since  $[x | z, \theta] = [x | z]$  (consequently the complete log-likelihood  $\ln([x, z | \theta])$  can be separated as  $\ln([x | z]) + \ln([z, | \theta])$ ) and the gamma random effects  $[z | \theta]$  belong to an exponential family. As a consequence, annex F shows that

$$\mathbb{E} \left| \frac{\partial^2 \ln([x, Z | \hat{\theta}])}{\partial \theta_i \partial \theta_j} \right| = \left| \frac{\partial^2 \ln([x, z | \hat{\theta}])}{\partial \theta_i \partial \theta_j} \right| = S \begin{pmatrix} -\psi'(\hat{a}) & \frac{1}{b} & 0 & 0 \\ \frac{1}{b} & -\frac{\hat{a}}{b^2} & 0 & 0 \\ 0 & 0 & -\psi'(\hat{c}) & \frac{1}{d} \\ 0 & 0 & \frac{1}{d} & \frac{\hat{c}}{d^2} \end{pmatrix}$$

As shown in Figure 20., given  $Y_s, Y_{s'}$  and  $\theta$ , the latent variables  $Z_s$  and  $Z_{s'}$  of two stratum  $s$  and  $s'$  are conditionnaly independent, therefore :

$$\text{Var}_{Z|x} \left( \frac{\partial \ln [x, Z | \theta]}{\partial \theta} \right) = \sum_{s=1}^S \text{Var}_{Z_s|x} \begin{pmatrix} \ln(\mu_s) \\ -\mu_s \\ \ln(\rho_s) \\ -\rho_s \end{pmatrix}$$

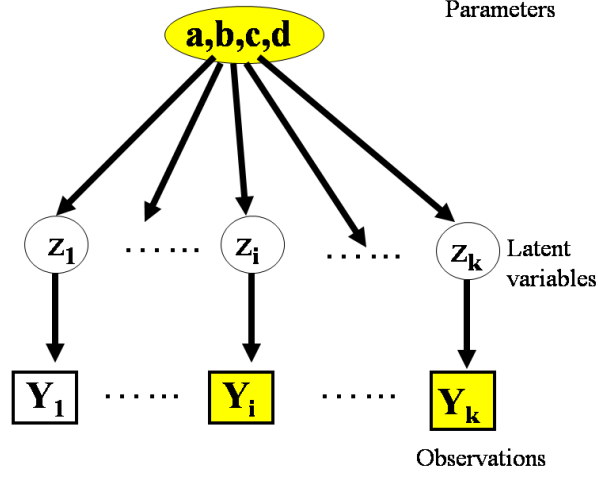


Figure 20: The random effects in each stratum are conditionally independent given the data and the set of parameters

To evaluate the variance of the score in stratum  $s$ , we will take advantage of successive conditioning due to the hierarchical structure depicted in Figure 2. Recalling that the latent variable  $Z_s$  includes, in addition to  $(\mu_s, \rho_s)$ , the vector  $\underline{N}_s$ , i-e the latent number of clumps for each record, the variance conditional decomposition formula gives:

$$\mathbb{V}ar_{Z_s|x} \begin{pmatrix} \ln(\mu_s) \\ -\mu_s \\ \ln(\rho_s) \\ -\rho_s \end{pmatrix} = \mathbb{E}_{\underline{N}_s|x} \left( \mathbb{V}ar \begin{pmatrix} \ln(\mu_s) \\ -\mu_s \\ \ln(\rho_s) \\ -\rho_s \end{pmatrix} \middle| \underline{N}_s \right) + \mathbb{V}ar_{\underline{N}_s|x} \left( \mathbb{E} \begin{pmatrix} \ln(\mu_s) \\ -\mu_s \\ \ln(\rho_s) \\ -\rho_s \end{pmatrix} \middle| \underline{N}_s \right)$$

So that we have

$$I_e(\hat{\theta}, x) = S \begin{pmatrix} -\psi'(\hat{a}) & \frac{1}{\hat{b}} & 0 & 0 \\ \frac{1}{\hat{b}} & -\frac{\hat{a}}{\hat{b}^2} & 0 & 0 \\ 0 & 0 & -\psi'(\hat{c}) & \frac{1}{\hat{d}} \\ 0 & 0 & \frac{1}{\hat{d}} & -\frac{\hat{c}}{\hat{d}^2} \end{pmatrix} + \sum_{s=1}^S (A_s + B_s)$$

with

$$A_s = \mathbb{E}_{\underline{\mathbf{N}}|x} \left( \text{Var} \left( \begin{array}{c} \ln(\mu_s) \\ -\mu_s \\ \ln(\rho_s) \\ -\rho_s \end{array} \middle| \underline{\mathbf{N}} \right) \right) \quad \text{and} \quad B_s = \text{Var}_{\underline{N}_s|x} \left( \mathbb{E} \left( \begin{array}{c} \ln(\mu_s) \\ -\mu_s \\ \ln(\rho_s) \\ -\rho_s \end{array} \middle| \underline{N}_s \right) \right).$$

Given  $\underline{N}_s$ ,  $\mu_s$  and  $\rho_s$  are independent. Moreover the *pdf*  $[\rho_s | \underline{N}_s, \underline{Y}_s, a, b, c, d]$  and  $[\mu_s | \underline{N}_s, \underline{Y}_s, a, b, c, d]$  are gamma and analytic expressions are available for the expectation and variance of the gamma sufficient statistics, as detailed in equations C.1 to C.3. The key functions of  $N_{s+}$  are  $(a_s', b_s', c_s', d_s') = (a + N_{s+}, b + D_{s+}, c + N_{s+}, d + Y_{s+})$  such that :

$$\mathbb{E} \left( \begin{array}{c} \ln(\mu_s) \\ -\mu_s \\ \ln(\rho_s) \\ -\rho_s \end{array} \middle| \underline{\mathbf{N}} \right) = \begin{pmatrix} \psi(a_s') - \ln(b_s') \\ -\frac{a_s'}{b_s'} \\ \psi(c_s') - \ln(d_s') \\ -\frac{c_s'}{d_s'} \end{pmatrix}$$

and then  $B_s$  is obtained by taking the covariance of this vector :

$$B_s = \text{Var}_{N_{s+}|\hat{\theta}, x} \left( \mathbb{E} \left( \begin{array}{c} \ln(\mu_s) \\ -\mu_s \\ \ln(\rho_s) \\ -\rho_s \end{array} \middle| \underline{\mathbf{N}}_{s+} \right) \right)$$

Given  $\underline{N}_s$  additional advantage is taken from the conditional independence of  $\rho_s$  and  $\mu_s$  as shown in Figure 21, .

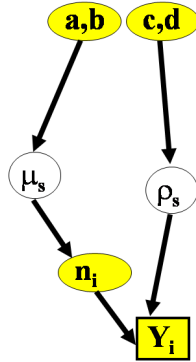


Figure 21: Given  $N$ ,  $\rho_s \perp \mu_s$



$$\text{Var} \begin{pmatrix} \ln(\mu_s) \\ -\mu_s \\ \ln(\rho_s) \\ -\rho_s \end{pmatrix} \Big| \underline{\mathbf{N}} = \begin{pmatrix} -\psi'(a') & \frac{1}{b'} & 0 & 0 \\ \frac{1}{b'} & -\frac{a'}{b'^2} & 0 & 0 \\ 0 & 0 & -\psi'(c') & \frac{1}{d'} \\ 0 & 0 & \frac{1}{d'} & \frac{-c'}{d'^2} \end{pmatrix}$$

607 and the expression for  $A_s$  follows easily.

## 608 F. Second derivative of the complete log-likelihood

Let us first recall the complete log likelihood of the model :

$$\begin{aligned} \ln [x, z | \theta] = & C_{-\theta} + (a - 1) \sum_{s=1}^S \ln \mu_s + Sa \ln b - b \sum_{s=1}^S \mu_s - S \ln \Gamma(a) \\ & + (c - 1) \sum_{s=1}^S \ln \rho_s + Sc \ln d - d \sum_{s=1}^S \rho_s - S \ln \Gamma(c) \end{aligned}$$

In the first derivative, the latent variables  $\boldsymbol{\mu}$  and  $\boldsymbol{\rho}$  appear not surprisingly only through their arithmetic or geometric means (sufficient statistics for the gamma pdf). Using standard notation  $\bar{\mu}$  for the arithmetic mean  $\frac{1}{S} \sum_{s=1}^S \mu_s$ , we have :

$$\begin{aligned} \frac{\partial \ln [x, z | \theta]}{\partial a} = S \left( \overline{\ln(\mu)} + \ln b - \psi(a) \right) & \quad \frac{\partial \ln [x, z | \theta]}{\partial c} = S \left( \overline{\ln(\rho)} + \ln d - \psi(c) \right) \\ \frac{\partial \ln [x, z | \theta]}{\partial b} = S \left( \frac{a}{b} - \bar{\mu} \right) & \quad \frac{\partial \ln [x, z | \theta]}{\partial d} = S \left( \frac{c}{d} - \bar{\rho} \right) \end{aligned}$$

609 The gradient of the complete log-likelihood (so-called the "score") may be split  
610 into two parts : the first one  $\Delta_\theta$  does not depend on the latent variable  $z$  while  
611 the other one  $\Delta_z$  gathers terms depending on  $z$  (and possibly of  $\theta$ ), i.e :

$$\left( \frac{\partial \ln [x, z | \hat{\theta}]}{\partial \theta} \right) = \Delta_\theta + \Delta_z$$

with

$$\Delta_\theta = S \begin{pmatrix} \ln b - \psi(a) \\ \frac{a}{b} \\ \ln d - \psi(c) \\ \frac{c}{d} \end{pmatrix} \quad \Delta_z = S \begin{pmatrix} \overline{\ln(\mu)} \\ -\bar{\mu} \\ \overline{\ln(\rho)} \\ -\bar{\rho} \end{pmatrix}$$

In addition here,  $\Delta_z$  does not contain terms with  $\theta$ , consequently the second

order derivatives are easy to obtain and don't involve the latent variable :

$$\begin{aligned} \frac{\partial^2 \ln [x, z | \theta]}{\partial a \partial a} &= -S\psi'(a) & \frac{\partial^2 \ln [x, z | \theta]}{\partial c \partial c} &= -S\psi'(c) \\ \frac{\partial^2 \ln [x, z | \theta]}{\partial a \partial b} &= \frac{S}{b} & \frac{\partial^2 \ln [x, z | \theta]}{\partial c \partial d} &= \frac{S}{d} \\ \frac{\partial^2 \ln [x, z | \theta]}{\partial b \partial b} &= -\frac{Sa}{b^2} & \frac{\partial^2 \ln [x, z | \theta]}{\partial d \partial d} &= \frac{-Sc}{d^2} \end{aligned}$$

## 612 G. Second derivative of the complete log-likelihood with discrete data

The complete log likelihood of the model, in the discrete case, reads :

$$\begin{aligned} \ln [x, z | \theta] &= C_{-\theta} + (a-1) \sum_{s=1}^S \ln \mu_s + Sa \ln b - b \sum_{s=1}^S \mu_s - S \ln \Gamma(a) \\ S \ln \left( \frac{\Gamma(c+d)}{\Gamma(c)\Gamma(d)} \right) &+ (c-1) \sum_{s=1}^S \ln p_s + (d-1) \sum_{s=1}^S \ln(1-p_s) \end{aligned}$$

In the first derivative, the latent variables  $\boldsymbol{\mu}$  and  $\boldsymbol{p}$  appear only through their arithmetic or geometric means (sufficient statistics for the gamma and beta *pdf*). Using standard notation  $\bar{\mu}$  for the arithmetic mean  $\frac{1}{S} \sum_{s=1}^S \mu_s$ , we have :

$$\begin{aligned} \frac{\partial \ln [x, z | \theta]}{\partial a} &= S \left( \overline{\ln(\mu)} + \ln b - \psi(a) \right) & \frac{\partial \ln [x, z | \theta]}{\partial c} &= S \left( \overline{\ln(p)} + \psi(c+d) - \psi(c) \right) \\ \frac{\partial \ln [x, z | \theta]}{\partial b} &= S \left( \frac{a}{b} - \bar{\mu} \right) & \frac{\partial \ln [x, z | \theta]}{\partial d} &= S \left( \overline{\ln(1-p)} + \psi(c+d) - \psi(d) \right) \end{aligned}$$

613 The gradient of the complete log-likelihood (so-called the "score") may be split  
614 into two parts : the first one  $\Delta_\theta$  does not depend on the latent variable  $z$  while  
615 the other one  $\Delta_z$  gathers terms depending on  $z$  (and possibly of  $\theta$ ), i.e :

$$\left( \frac{\partial \ln [x, z | \hat{\theta}]}{\partial \theta} \right) = \Delta_\theta + \Delta_z$$

with

$$\Delta_\theta = S \begin{pmatrix} \ln b - \psi(a) \\ \frac{a}{b} \\ \psi(c+d) - \psi(c) \\ \psi(c+d) - \psi(d) \end{pmatrix} \quad \Delta_z = S \begin{pmatrix} \overline{\ln(\mu)} \\ -\bar{\mu} \\ \overline{\ln(p)} \\ \overline{\ln(1-p)} \end{pmatrix}$$

In addition here,  $\Delta_z$  does not contain terms with  $\theta$ , consequently the second order derivatives are easy to obtain and don't involve the latent variable; with  $Z$  standing for all the hidden variables i.e  $\underline{Z} = (\underline{N}, \underline{\mu}, \underline{p})$ :

$$\left| \frac{\partial^2 \ln([x, z | \hat{\theta}])}{\partial \theta_i \partial \theta_j} \right| = S \begin{pmatrix} -\psi'(\hat{a}) & \frac{1}{\hat{b}} & 0 & 0 \\ \frac{1}{\hat{b}} & -\frac{\hat{a}}{\hat{b}^2} & 0 & 0 \\ 0 & 0 & -\psi'(\hat{c}) + \psi'(\hat{c} + \hat{d}) & \psi'(\hat{c} + \hat{d}) \\ 0 & 0 & \psi'(\hat{c} + \hat{d}) & -\psi'(\hat{d}) + \psi'(\hat{c} + \hat{d}) \end{pmatrix}$$

As shown in Figure 20 for the continuous case, given  $Y_s, Y_{s'}$  and  $\theta$ , the latent variables  $Z_s$  and  $Z_{s'}$  of two strata  $s$  and  $s'$  are conditionnaly independent, therefore :

$$\mathbb{V}ar_{Z|x} \left( \frac{\partial \ln [x, Z | \theta]}{\partial \theta} \right) = \sum_{s=1}^S \mathbb{V}ar_{Z_s|x} \begin{pmatrix} \ln(\mu_s) \\ -\mu_s \\ \ln(p_s) \\ \ln(1 - p_s) \end{pmatrix}$$

To evaluate the variance of the score in stratum  $s$ , we will take advantage from successive conditioning due to the hierarchical structure depicted in Figure 2 still true for the discrete case. The variance conditional decomposition formula gives:

$$\mathbb{V}ar_{Z_s|x} \begin{pmatrix} \ln(\mu_s) \\ -\mu_s \\ \ln(p_s) \\ -\rho_s \end{pmatrix} = \mathbb{E}_{\underline{N}_s|x} \left( \mathbb{V}ar \begin{pmatrix} \ln(\mu_s) \\ -\mu_s \\ \ln(p_s) \\ \ln(1 - p_s) \end{pmatrix} \middle| \underline{N}_s \right) + \mathbb{V}ar_{\underline{N}_s|x} \left( \mathbb{E} \begin{pmatrix} \ln(\mu_s) \\ -\mu_s \\ \ln(p_s) \\ \ln(1 - p_s) \end{pmatrix} \middle| \underline{N}_s \right)$$

So that we have

$$I_e(\hat{\theta}, x) = S \begin{pmatrix} -\psi'(\hat{a}) & \frac{1}{\hat{b}} & 0 & 0 \\ \frac{1}{\hat{b}} & -\frac{\hat{a}}{\hat{b}^2} & 0 & 0 \\ 0 & 0 & -\psi'(\hat{c}) + \psi'(\hat{c} + \hat{d}) & \psi'(\hat{c} + \hat{d}) \\ 0 & 0 & \psi'(\hat{c} + \hat{d}) & -\psi'(\hat{d}) + \psi'(\hat{c} + \hat{d}) \end{pmatrix} + \sum_{s=1}^S (A_s + B_s)$$

with

$$A_s = \mathbb{E}_{\underline{N}|x} \left( \mathbb{V}ar \begin{pmatrix} \ln(\mu_s) \\ -\mu_s \\ \ln(p_s) \\ \ln(1 - p_s) \end{pmatrix} \middle| \underline{N} \right) \quad \text{and} \quad B_s = \mathbb{V}ar_{\underline{N}_s|x} \left( \mathbb{E} \begin{pmatrix} \ln(\mu_s) \\ -\mu_s \\ \ln(p_s) \\ \ln(1 - p_s) \end{pmatrix} \middle| \underline{N}_s \right).$$

Given  $\underline{N}_s$ ,  $\mu_s$  and  $\rho_s$  are independent. Moreover the *pdf*  $[\rho_s | \underline{N}_s, \underline{Y}_s, a, b, c, d]$  and  $[p_s | \underline{N}_s, \underline{Y}_s, a, b, c, d]$  are gamma and beta so that analytic expressions are available

for the expectation and variance of the gamma sufficient statistics, as detailed in equations C.1 to C.3. The key functions of  $N_{s+}$  are  $(a_s!, b_s!, c_s!, d_s!) = (a + N_{s+}, b + D_{s+}, c + N_{s+}, d + Y_{s+} - N_{s+})$  such that :

$$\mathbb{E} \left( \begin{array}{c} \ln(\mu_s) \\ -\mu_s \\ \ln(p_s) \\ \ln(1-p_s) \end{array} \middle| \underline{\mathbf{N}} \right) = \left( \begin{array}{c} \psi(a'_s) - \ln(b'_s) \\ -\frac{a'_s}{b'_s} \\ \psi(c'_s) - \psi(c'_s + d'_s) \\ \psi(d'_s) - \psi(c'_s + d'_s) \end{array} \right)$$

and then the matrix  $B_s$  is obtained by taking the covariance of this vector. Given  $\underline{N}_s$  additional advantage is taken from the conditional independence of  $p_s$  and  $\mu_s$  (as shown on Figure 21 for the continuous case).

$$\text{Var} \left( \begin{array}{c} \ln(\mu_s) \\ -\mu_s \\ \ln(\rho_s) \\ -\rho_s \end{array} \middle| \underline{\mathbf{N}} \right) = \left( \begin{array}{cccc} -\psi'(a') & \frac{1}{b'} & 0 & 0 \\ \frac{1}{b'} & -\frac{a'}{b'^2} & 0 & 0 \\ 0 & 0 & \psi'(c'_s) - \psi'(c'_s + d'_s) & -\psi'(c'_s + d'_s) \\ 0 & 0 & -\psi'(c'_s + d'_s) & \psi'(d'_s) - \psi'(c'_s + d'_s) \end{array} \right)$$

616 and the expectation to obtain  $A_s$  is performed via importance sampling.

To sum it up

$$I_e(\theta) = -\frac{\partial^2 \ln [\underline{\mathbf{Y}}|\theta]}{\partial \theta_i \partial \theta_j} \quad (\text{G.1})$$

At the maximum likelihood estimator  $\hat{\theta}$ , the following equality occurs :

$$I_e(\hat{\theta}, \underline{\mathbf{Y}}) = S \left( \begin{array}{cccc} -\psi'(\hat{a}) & \frac{1}{\hat{b}} & 0 & 0 \\ \frac{1}{\hat{b}} & -\frac{\hat{a}}{\hat{b}^2} & 0 & 0 \\ 0 & 0 & -\psi'(\hat{c}) + \psi'(\hat{c} + \hat{d}) & \psi'(\hat{c} + \hat{d}) \\ 0 & 0 & \psi'(\hat{c} + \hat{d}) & -\psi'(\hat{d}) + \psi'(\hat{c} + \hat{d}) \end{array} \right) + \sum_{s=1}^S (A_s + B_s) \quad (\text{G.2})$$

with

$$A_s = \left( \begin{array}{cccc} \mathbb{E}_{\nu_s}(\psi'(a'_s)) & \frac{-1}{b'_s} & 0 & 0 \\ \frac{-1}{b'_s} & \frac{\mathbb{E}_{N_{s+}|\underline{\mathbf{Y}}, \hat{\theta}}(a'_s)}{b'^2_s} & 0 & 0 \\ 0 & 0 & \mathbb{E}_{\nu_s}(\psi'(c'_s) - \psi'(c'_s + d'_s)) & -\mathbb{E}_{\nu_s}(\psi'(c'_s + d'_s)) \\ 0 & 0 & -\mathbb{E}_{\nu_s}(\psi'(c'_s + d'_s)) & \mathbb{E}_{\nu_s}(\psi'(d'_s) - \psi'(c'_s + d'_s)) \end{array} \right)$$

and

$$B_s = \text{Var}_{N_{s+}|\hat{\theta},x} \begin{pmatrix} \psi(a'_s) - \ln(b'_s) \\ -\frac{a'_s}{b'_s} \\ \psi(c'_s) - \psi(c'_s + d'_s) \\ \psi(d'_s) - \psi(c'_s + d'_s) \end{pmatrix}$$

617 where  $a'_s = \hat{a} + N_{s+}$ ,  $b'_s = \hat{b} + D_{s+}$ ,  $c'_s = \hat{c} + N_{s+}$  and  $d'_s = \hat{d} + Y_{s+} - N_{s+}$  ( $b'_s$   
618 is the only term that is not a function of  $N_{s+}$ , thus behaving like a constant with  
619 regards to the  $\text{Var}_{N_{s+}|\hat{\theta},x}$  operator)

## 620 H. The discrete algorithm

621 If we adapt bluntly from the continuous version, the algorithm would write

- 622 1. Generate  $N_i^{(g)} = 0$  wherever  $y_{i=0}$  for  $i = I - I^+ + 1, \dots, I$ .
2. Generate a value of  $N_+$  according to

$$N_+ \propto \frac{\Gamma(a' + N_+) \Gamma(c' + N_+) \Gamma(d' + Y_+ - N_+) D_+^{N_+}}{(b' + D_+)^{a'+N_+} \prod_{j=1}^{I^+} \Gamma\left(N_+ \frac{Y_j D_j}{(YD)_+}\right)}$$

- 623 3. Generate each  $N_i$  for  $i = 1, \dots, I^+$ , so that the vector  $\underline{N}$  is distributed  
624 according to a multivariate hypergeometric Fisher distribution [17] given by

$$[\underline{N}|N_+] = \frac{g(\underline{N}; N_+, \underline{Y}, \underline{D}/D_+)}{K_{N_+}}$$

with

$$g(\underline{N}; N_+, \underline{Y}, \underline{D}) = \prod_{i=I^*+1}^I \binom{Y_j}{N_j} (D_j/D_+)^{N_j},$$

$$K_{N_+} = \sum_{y \in \mathcal{S}} g(\underline{y}; N_+, \underline{Y}, \underline{D}),$$

and

$$\mathcal{S} = \left\{ \underline{N} \in \mathbb{Z}_+^{I^+} \mid \sum_{i=I^*+1}^I N_i = N_+ \right\}.$$

4. Associate to the vector the weight

$$w^{(g)} = K_{N_+^{(g)}} \prod_{i=I^*}^I \frac{\Gamma\left(N_+^{(g)} \frac{Y_j D_j}{(YD)_+}\right)}{\Gamma(N_j)}.$$

Importance Sampling relying this time on the multivariate hypergeometric distribution seems to stand naturally as the core of the algorithm to evaluate (3.23). But during our first trials, the above adaptation of the continuous version performed very badly, leading to a large variance of the importance weights, i.e. a degeneracy phenomenon that would put the all weight onto a very few contributing particles. In order to put more weight onto particles that have a good chance to efficiently attain the target distribution, a mixture was chosen as the importance distribution for a modified algorithm. The idea is similar in spirit to the auxiliary particle filtering of [20]. More precisely, the first step consists of determining an approximate mean of  $N_{s+}$  in stratum  $s$ , denoted  $N_{s+}^{(ref)}$ . One draws a L-sample of  $N_{s+}$  according to

$$g(N_+) \propto \frac{\Gamma(a' + N_+) \Gamma(c' + N_+) \Gamma(d' + y_+ - N_+) D_+^{N_+}}{\Gamma(b' + D_+)^{a'+N_+} \Gamma(N_+ + 1) \Gamma(N_+) \Gamma(Y_+ - N_+ + 1)}$$

The  $g$  distribution corresponds to the conditional distribution of  $N_+$  given the sum of the data collected in stratum  $s$  but ignoring the individual records.  $N_{s+}^{(ref)}$  is given by the mean over a sample that is

$$N_{s+}^{(ref)} = \frac{1}{L} \sum N_+^{(i)}$$

625 and provides a good estimation of the location of  $N_{s+}$ . As previously we omit the  
626 index  $s$  to make the reading easier. Subsequently, the following algorithm relies  
627 on independent but non identically distributed simulations :

- 628 1. Generate  $N_i^{(g)} = 0$  wherever  $y_i = 0$  for  $i = I - I^+ + 1, \dots, I$ .
- 629 2. Draw  $\mu^{(g)} \sim \Gamma(a' + N_+^{(ref)}, b' + D_+)$  and  $p^{(g)} \sim \beta(c' + N_{s+}^{(ref)}, d' + Y_{s+} - N_{s+}^{(ref)})$
3. Given  $\mu^{(g)}$  and  $\rho^{(g)}$ , draw  $N_{sk}^{(g)} \sim [N_{sk} | \mu^{(g)}, p^{(g)}, y_{sk}]$  that is :

$$[N_i^{(g)} = k] = K_i \left( \frac{\mu^{(g)} p^{(g)} D_i}{1 - p^{(g)}} \right)^{N_i} \frac{1}{\Gamma(N_i) \Gamma(Y_i - N_i + 1) \Gamma(N_i + 1)} \mathbb{1}_{\{0 < N_{sk} \leq Y_{si}\}},$$

630 where  $K_i$  denotes the normalizing constant.

4. Compute the weight of each particle  $g$  using

$$w^{(g)} = \prod_{i=1}^{I^+} \frac{\Gamma(N_i + 1)}{K_i (\mu^{(g)} p^{(g)})^{N_i}} \left( \frac{\Gamma(a' + N_{s+}) \Gamma(N_{s+} + c') \Gamma(Y_+ - N_{s+} + d')}{(b' + D_{s+})^{N_{s+}}} \right)$$